

FTUAM 00/20
 IFT-UAM/CSIC 00/42
 KA-TP-10-2001
 hep-ph/0105097
 March 2001

SUSY-QCD decoupling properties in $H^+ \rightarrow t\bar{b}$ decay

María J. Herrero^a, Siannah Peñaranda^b * and David Temes^a †

^a *Departamento de Física Teórica*

Universidad Autónoma de Madrid, Cantoblanco, 28049 Madrid, Spain.

^b *Institut für Theoretische Physik*

Universität Karlsruhe, Kaiserstraße 12, D-76128 Karlsruhe.

Abstract

The SUSY-QCD radiative corrections to the $\Gamma(H^+ \rightarrow t\bar{b})$ partial decay width are analyzed within the Minimal Supersymmetric Standard Model at the one-loop level, $\mathcal{O}(\alpha_s)$, and in the decoupling limit. We present the analytical expressions of these corrections in the large SUSY masses limit and study the decoupling behaviour of these corrections in various limiting cases. We find that if the SUSY mass parameters are large and of the same order, the one loop SUSY-QCD corrections *do not decouple*. The non-decoupling contribution is enhanced by $\tan\beta$ and therefore large corrections are expected in the large $\tan\beta$ limit. In contrast, we also find that the SUSY-QCD corrections decouple if the masses of either the squarks or the gluinos are separately taken large.

*On leave from Departamento de Física Teórica, Universidad Autónoma de Madrid, Madrid, Spain.

†electronic addresses: herrero@delta.ft.uam.es, siannah@particle.uni-karlsruhe.de, temes@delta.ft.uam.es

1 Introduction

Despite its tremendous success in the agreement between the Standard Model (SM) predictions and the experimental data, this model contains a variety of theoretical problems which cannot be solved without the introduction of some new physics. Here we will be concerned about two candidates for physics beyond the SM: Supersymmetry (SUSY) and Extended Higgs Sectors.

The minimal extension of the SM Higgs sector is a two Higgs doublet model (2HDM). This model predicts three neutral Higgs bosons, two CP even (h^0 , H^0) one CP odd (A^0), and two charged bosons (H^\pm); and includes one parameter, $\tan\beta$, defined as the ratio of the two Higgs vacuum expectation values (*vevs*) [1]. On the other hand, constructing a Minimal Supersymmetric extension of the Standard Model (MSSM) [2] implies a two Higgs doublet sector, with the same spectrum as in a 2HDM extension of the SM but with constrained Yukawa and Higgs self-couplings. To be more specific, the MSSM Higgs sector belongs to the so-called type II models, in which one Higgs doublet couples to u-like quarks and the other one to d-like quarks [1].

Looking for non-SM effects on the Higgs phenomenology of these extended models we realize that, while both the neutral Higgs bosons may not be easily distinguishable from that of the SM, the discovery of H^\pm and the determination of its mass and couplings are expected to be a very clear signal of physics beyond the SM in the Higgs sector. This is the main reason why the search for charged Higgs bosons is one of the major tasks at present and future colliders.

Concerning the present experimental search of charged Higgs bosons the situation is as follows. LEP2 has set a model independent lower limit on the H^+ mass, $m_{H^+} \geq 77.4$ GeV [3]. At Tevatron, the CDF and D0 collaborations have searched for H^\pm bosons in top decays through the process $p\bar{p} \rightarrow t\bar{t}$, with at least one of the top quarks decaying via $t \rightarrow H^+ b$, leading to an excess of τ due to the $H^+ \rightarrow \tau^+ \nu$ decay; they have excluded regions with light H^+ and large values of $\tan\beta$, for example if $M_{H^+} = 100$ GeV, $\tan\beta \geq 60$ is excluded [4]. In any case, the allowed region in the $(\tan\beta - M_{H^\pm})$ plane can be significantly modified by quantum corrections [5].

Here we consider the case of a heavy charged Higgs boson, $M_{H^+} \geq m_t + m_b$. In this case H^+ bosons will decay mostly into $t\bar{b}$ pairs with approximately $BR \geq 85\%$ [6], depending on the values of $\tan\beta$ and M_{H^+} . On the other hand the two main H^+ production subprocesses which will provide sizeable cross sections at LHC are: $g\bar{b} \rightarrow \bar{t}H^+$ [7] and $gg \rightarrow \bar{t}H^+ b$ [8]. Thus, the importance of the $H^+ \rightarrow t\bar{b}$ decay comes in two directions: it is the dominant decay over most of the parameter space and its associated effective vertex $H^+ t\bar{b}$ appears in the two main production processes.

Once a charged Higgs Boson is found, a precise determination of its couplings to SM particles, which are sensitive to radiative corrections, can give us indirect information about extra new physics beyond the SM. In particu-

lar one may wonder if the H^\pm is itself an indirect signal of supersymmetry and explore if its corrected couplings to SM fermions are like in the MSSM or like in a non-SUSY 2HDM. In order to compare the predictions in the MSSM and in the 2HDM extension of the SM for these couplings, we assume here the most pessimistic scenario where the genuine supersymmetric spectrum is very heavy as compared with the electroweak scale. This situation corresponds to the decoupling of supersymmetric particles from the rest of the MSSM spectrum, namely, the SM particles and the MSSM Higgs sector. In this decoupling limit the SUSY particles can not be produced directly in the colliders and we are constrained to indirect searches for SUSY. Here we will look for indirect heavy SUSY signals through their effect on radiative corrections to the $H^+ \rightarrow t\bar{b}$ decay.

Recent works on the decoupling limit have shown that all the genuine heavy SUSY particles and heavy Higgs bosons (H^0 , A^0 and H^\pm) of the MSSM decouple, at one-loop order, from the low-energy electroweak gauge bosons physics [9]. On the other hand, concerning the Higgs physics, the decoupling behaviour of the one-loop SUSY-QCD radiative corrections to the $\Gamma(h^0 \rightarrow b\bar{b})$ partial width have been studied in [10]. There it was found that, for fixed masses of the extra Higgses (H^0 , A^0 and H^\pm), the SUSY-QCD corrections from nearly heavy degenerate gluinos and squarks do not decouple in the $\Gamma(h^0 \rightarrow b\bar{b})$ decay width. The SUSY-QCD corrections to the main Higgs bosons and top decays have also been analyzed in [11].

In this paper we study the MSSM radiative corrections to the $H^+ \rightarrow t\bar{b}$ decay width at one loop level and to leading order in α_s , and we analyze their behaviour in the decoupling limit of heavy SUSY particles. These corrections come from the SUSY-QCD [12, 13] and pure QCD sectors [14] and are known to provide the dominant contributions to the $\Gamma(H^+ \rightarrow t\bar{b})$ partial width. The QCD corrections range from +10% to -50% and the SUSY-QCD corrections can be even larger in a large region of the SUSY parameter space. Since a 2HDM extension of the SM has no SUSY-QCD contributions to $H^+ \rightarrow t\bar{b}$, one could use these corrections in order to distinguish between the MSSM and the 2HDM.

Here we analyze the full diagrammatic formulae for the on-shell one-loop SUSY-QCD corrections to the $H^+ \rightarrow t\bar{b}$ decay. We perform expansions in inverse powers of the SUSY masses in order to examine the decoupling behavior when these masses are large compared to the electroweak scale. The SUSY-QCD corrections depend on a number of different MSSM mass parameters, and we will see that the relative sizes of these parameters do affect qualitatively the decoupling behaviour. To remain as model-independent as possible, we make no assumptions about relations among the MSSM parameters that may arise from grand unification or specific SUSY-breaking scenarios. We consider the soft-SUSY-breaking parameters and the μ parameter as unknown parameters whose magnitudes are all of order 1 TeV. We examine in great detail the case of large $\tan\beta$, for which the SUSY-QCD corrections are enhanced. This enhancement gives rise to a significant

one-loop correction, even for moderate and large values of the SUSY masses.

This paper is organized as follows. In Section 2 we define our notation and briefly review the Higgs and squark sectors of the MSSM. In Section 3 we review the exact one loop result for the SUSY-QCD corrections to the $H^+ \rightarrow t\bar{b}$ partial decay width. In Section 4 we derive analytic expressions for these corrections in the limit of large SUSY masses and for several extreme squark mixing cases. We also analyze the decoupling of the SUSY-QCD corrections for various hierarchies of mass parameters, and compare the analytic approximations to the exact one-loop result. Finally, we summarize our conclusions in Section 5.

2 MSSM Higgs and squark sectors

In the MSSM there are two isospin Higgs doublets containing eight degrees of freedom. After the electroweak symmetry-breaking mechanism, three of these eight degrees of freedom are absorbed by the Z and W^\pm gauge bosons, leading to the existence of five physical Higgs particles. These consist of two CP-even neutral scalar particles h^0 , H^0 , one CP-odd neutral pseudoscalar particle A^0 and two charged scalar particles H^\pm . Due to supersymmetry, the parameters of the Higgs sector are constrained and, at tree-level, it turns out that the Higgs masses and mixing angle depend on just two unknown parameters. These are commonly chosen to be the mass of the CP-odd neutral Higgs boson, M_A , and the ratio of the *vevs* of the two Higgs doublets, $\tan\beta = v_2/v_1$. The Higgs bosons masses at tree level, in terms of these parameters, are given by:

$$M_{H^\pm}^2 = M_A^2 + M_W^2$$

$$M_{H^0, h^0}^2 = \frac{1}{2} \left[M_A^2 + M_Z^2 \pm \sqrt{(M_A^2 + M_Z^2)^2 - 4M_A^2 M_Z^2 \cos^2 2\beta} \right]. \quad (1)$$

We choose a convention where the *vevs* are positive so that $0 < \beta < \pi/2$. The mixing angle in the neutral sector is given at tree-level by:

$$\tan 2\alpha = \tan 2\beta \frac{M_A^2 + M_Z^2}{M_A^2 - M_Z^2}. \quad (2)$$

In the conventions employed here, $-\pi/2 < \alpha < 0$.

We now discuss the parameters of the third generation squark sector. For simplicity, we assume here that there is no intergenerational flavour mixing. The tree-level stop and sbottom squared-mass matrices are:

$$\mathcal{M}_t^2 = \begin{pmatrix} M_L^2 & m_t X_t \\ m_t X_t & M_R^2 \end{pmatrix}, \quad (3)$$

$$\mathcal{M}_{\tilde{b}}^2 = \begin{pmatrix} M_L'^2 & m_b X_b \\ m_b X_b & M_R'^2 \end{pmatrix}, \quad (4)$$

where:

$$\begin{aligned}
M_L^2 &= M_{\tilde{Q}}^2 + m_t^2 + \cos 2\beta (1/2 - 2/3 s_W^2) M_Z^2 \\
M_R^2 &= M_{\tilde{U}}^2 + m_t^2 + 2/3 \cos 2\beta s_W^2 M_Z^2 \\
X_t &= A_t - \mu \cot \beta \\
M_L'^2 &= M_{\tilde{Q}}^2 + m_b^2 - \cos 2\beta (1/2 - 1/3 s_W^2) M_Z^2 \\
M_R'^2 &= M_{\tilde{D}}^2 + m_b^2 - 1/3 \cos 2\beta s_W^2 M_Z^2 \\
X_b &= A_b - \mu \tan \beta,
\end{aligned} \tag{5}$$

and $s_W \equiv \sin \theta_W$. The parameters $M_{\tilde{Q}}$, $M_{\tilde{D}}$ and $M_{\tilde{U}}$ are the soft-SUSY-breaking masses for the third-generation SU(2) squark doublet $\tilde{Q} = (\tilde{t}_L, \tilde{b}_L)$ and the singlets $\tilde{D} = \tilde{b}_R$ and $\tilde{U} = \tilde{t}_R$, respectively. $A_{b,t}$ are the corresponding soft-SUSY-breaking trilinear couplings and μ is the bilinear coupling of the two Higgs doublet. The squarks (sbottom and stop) mass eigenstates are given by:

$$\begin{pmatrix} \tilde{q}_1 \\ \tilde{q}_2 \end{pmatrix} = (R^{(q)})^{-1} \begin{pmatrix} \tilde{q}_L \\ \tilde{q}_R \end{pmatrix}, \tag{6}$$

where

$$R^{(q)} = \begin{pmatrix} \cos \theta_{\tilde{q}} & -\sin \theta_{\tilde{q}} \\ \sin \theta_{\tilde{q}} & \cos \theta_{\tilde{q}} \end{pmatrix}. \tag{7}$$

The stop and sbottom mass eigenvalues are given by¹:

$$\begin{aligned}
M_{\tilde{t}_{1,2}}^2 &= \frac{1}{2} \left[M_L^2 + M_R^2 \pm \sqrt{(M_L^2 - M_R^2)^2 + 4m_t^2 X_t^2} \right], \\
M_{\tilde{b}_{1,2}}^2 &= \frac{1}{2} \left[M_L'^2 + M_R'^2 \pm \sqrt{(M_L'^2 - M_R'^2)^2 + 4m_b^2 X_b^2} \right].
\end{aligned} \tag{8}$$

And the mixing angles $\theta_{\tilde{q}}$ ($q = t, b$) are given by:

$$\begin{aligned}
\cos 2\theta_{\tilde{t}} &= \frac{M_L^2 - M_R^2}{M_{\tilde{t}_1}^2 - M_{\tilde{t}_2}^2}, & \cos 2\theta_{\tilde{b}} &= \frac{M_L'^2 - M_R'^2}{M_{\tilde{b}_1}^2 - M_{\tilde{b}_2}^2}, \\
\sin 2\theta_{\tilde{q}} &= \frac{2m_q X_q}{M_{\tilde{q}_1}^2 - M_{\tilde{q}_2}^2}.
\end{aligned} \tag{9}$$

Concerning the experimental bounds on the SUSY and Higgs masses that are relevant for this work, we briefly summarize next the present situation. As mentioned before, from combined searches of charged Higgs bosons at LEP one gets a general lower limit of $M_{H^+} \geq 77.4$ GeV [3], valid at the 95% C.L. and for any value of the branching ratio $B(H^+ \rightarrow \tau^+ \nu)$. On the other hand, from absence of signals in direct searches at the Tevatron [15], the sbottoms must be heavier than about 140 GeV, assuming that the mass of the lightest neutralino $\tilde{\chi}_1^0$ is less than half the mass of the lighter sbottom. If

¹Note that in our convention, $M_{\tilde{t}_1} > M_{\tilde{t}_2}$ and $M_{\tilde{b}_1} > M_{\tilde{b}_2}$

$m_{\tilde{\chi}_1^0} = 40$ GeV the maximum excluded value for the scalar top mass is about 110 GeV at the 95% C.L.. For heavier neutralinos, the Tevatron searches lose efficiency. In this region the direct searches at LEP [16] place a lower bound on the sbottom masses of about 91 GeV under the assumption of a dominant $\tilde{b} \rightarrow b\tilde{\chi}_1^0$ decay. For $\tilde{t} - \tilde{\chi}_1^0$ mass splittings in the range from 6 to 40 GeV, *i.e.*, a region not accessible to the Tevatron searches, the lower limit on scalar top mass is 83 GeV, independently of the \tilde{t} mixing angle. All these lower limit results are at 95% C.L.. Finally, the limits on the gluino mass $M_{\tilde{g}}$ are more model-dependent. If one assumes relations between the gaugino masses such that they unify at the GUT scale, then $M_{\tilde{g}}$ is constrained from direct searches at the Tevatron to be greater than 173 GeV, independently of the squark masses [17].

3 $H^+ \rightarrow t\bar{b}$ partial decay width

The $H^+ \rightarrow t\bar{b}$ partial decay width at tree level is determined by the interaction Lagrangian describing the $H^+ t\bar{b}$ vertex, which is given by [18]:

$$\mathcal{L}_{Htb} = \frac{g V_{tb}}{\sqrt{2} M_W} H^+ \bar{t} [m_t \cot \beta P_L + m_b \tan \beta P_R] b + \text{h.c.}, \quad (10)$$

where $P_{L,R} = 1/2(1 \mp \gamma_5)$ are the chirality projection operators and V_{tb} is the corresponding CKM matrix element. Here we do not consider mixing between different families and we set $V_{tb} = 1$.

In this work we are interested in the dominant radiative corrections to the tree-level partial decay width $H^+ \rightarrow t\bar{b}$, which are known to come from QCD loops corrections. The leading corrections at one-loop level and to order α_s in the context of the MSSM were computed in [12–14]. They included the pure QCD corrections from quarks and gluons and the genuine SUSY-QCD corrections from gluinos and squarks. The standard QCD corrections were first computed in [14] and can be large, ranging from +10% to -50% with respect to the tree level contribution. The SUSY-QCD corrections, computed by using a diagrammatic approach in [12, 13], have been found to be comparable or even larger than the standard QCD contributions in a large region of the SUSY parameter space.

For completeness, and since the SUSY-QCD corrections are our starting point in order to study their behaviour in the large SUSY mass limit, we have reproduced the results in [12, 13] and we present in the following a short summary of the most relevant analytical expressions.

Following the standard renormalization procedure, there are two kinds of contributions to the partial decay width: one coming from the loop diagrams and another one coming from the counterterms. Taking this into account, we can write the $H^+ \rightarrow t\bar{b}$ partial decay width at the one-loop level and to

order α_s in the following way²:

$$\Gamma_1(H^+ \rightarrow t\bar{b}) = \Gamma_0(H^+ \rightarrow t\bar{b})(1 + 2\Delta^{\text{loops}} + 2\Delta^{\text{CT}}), \quad (11)$$

where Γ_1 is the one-loop partial width, Γ_0 is the tree-level partial width and Δ^{loops} and Δ^{CT} provide the corrections coming from the one-loop diagrams and from the counterterms, respectively.

Since the renormalization of the Higgs wave function, Higgs mass, the *vevs* (and hence $\tan\beta$) and the parameters g and M_W receive no $\mathcal{O}(\alpha_s)$ corrections at one-loop, the counterterms contribution originate just from the renormalization of the quark wave functions and quark masses. The corresponding expression for Δ^{CT} is:

$$\Delta^{\text{CT}} = \frac{U_t}{D} \left(\frac{\delta m_t}{m_t} + \frac{1}{2} \delta Z_L^b + \frac{1}{2} \delta Z_R^t \right) + \frac{U_b}{D} \left(\frac{\delta m_b}{m_b} + \frac{1}{2} \delta Z_L^t + \frac{1}{2} \delta Z_R^b \right), \quad (12)$$

where:

$$\begin{aligned} D &= (M_{H^+}^2 - m_t^2 - m_b^2)(m_t^2 \cot^2 \beta + m_b^2 \tan^2 \beta) - 4m_t^2 m_b^2, \\ U_t &= (M_{H^+}^2 - m_t^2 - m_b^2)m_t^2 \cot^2 \beta - 2m_t^2 m_b^2, \\ U_b &= (M_{H^+}^2 - m_t^2 - m_b^2)m_b^2 \tan^2 \beta - 2m_t^2 m_b^2. \end{aligned} \quad (13)$$

We use the on-shell renormalization scheme as defined in [19]. The contributions from the counterterms can be written in this scheme in terms of the bottom and top self-energies as follows:

$$\begin{aligned} \frac{\delta m_{(t,b)}}{m_{(t,b)}} + \frac{1}{2} \delta Z_L^{(b,t)} + \frac{1}{2} \delta Z_R^{(t,b)} &= \Sigma_S^{(t,b)}(m_{(t,b)}^2) + \frac{1}{2} \Sigma_L^{(t,b)}(m_{(t,b)}^2) - \frac{1}{2} \Sigma_L^{(b,t)}(m_{(b,t)}^2) \\ - \frac{m_t^2}{2} \left[\Sigma_L^{t'}(m_t^2) + \Sigma_R^{t'}(m_t^2) + 2\Sigma_S^{t'}(m_t^2) \right] - \frac{m_b^2}{2} \left[\Sigma_L^{b'}(m_b^2) + \Sigma_R^{b'}(m_b^2) + 2\Sigma_S^{b'}(m_b^2) \right] \end{aligned} \quad (14)$$

As we have already mentioned, in the present work we focus on the contributions to Δ^{loops} and Δ^{CT} coming from the SUSY-QCD sector:

$$\Delta_{\text{SQCD}} = \Delta_{\text{SQCD}}^{\text{loops}} + \Delta_{\text{SQCD}}^{\text{CT}} \quad (15)$$

where we use the short notation SQCD for SUSY-QCD.

The SUSY-QCD contributions to the $H^+ \rightarrow t\bar{b}$ decay width come from diagrams involving the exchange of virtual gluinos (\tilde{g}), sbottoms (\tilde{b}) and stops (\tilde{t}). The diagrams that contribute to the vertex corrections and quark

²The factor 2 used here is a convention such that the corresponding correction to the effective coupling is:

$$g_{H^+ b\bar{t}}^{\text{1-loop}} = g_{H^+ b\bar{t}}^{\text{tree}}(1 + \Delta^{\text{loops}} + \Delta^{\text{CT}}).$$

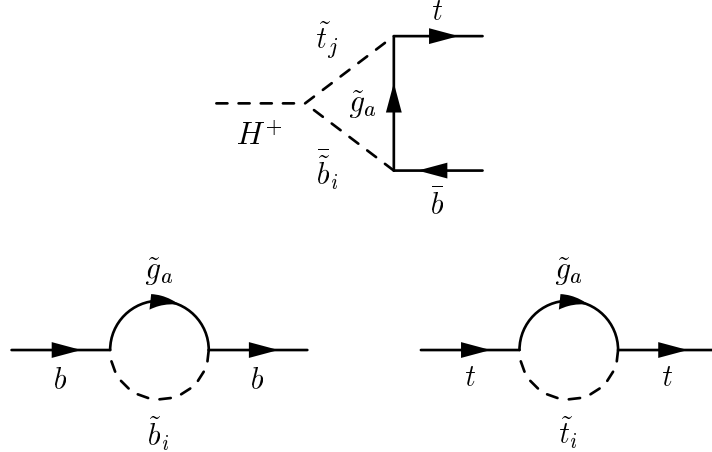


Figure 1: Diagrams corresponding to the vertex correction and quark self-energies that contribute to Δ_{SQCD} .

self energies are shown in Fig. 1. The contribution from the one-loop vertex diagrams are given by:

$$\Delta_{SQCD}^{loops} = \frac{U_t}{D} H_t + \frac{U_b}{D} H_b, \quad (16)$$

where:

$$\begin{aligned} H_t &= -\frac{2\alpha_s}{3\pi} \frac{G_{ab}^*}{m_t \cot \beta} [m_t R_{1b}^{(t)} R_{1a}^{(b)*} (C_{11} - C_{12}) + m_b R_{2b}^{(t)} R_{2a}^{(b)*} C_{12} \\ &\quad + M_{\tilde{g}} R_{2b}^{(t)} R_{1a}^{(b)*} C_0] (m_t^2, M_{H^+}^2, m_b^2, M_{\tilde{g}}^2, M_{\tilde{t}_b}^2, M_{\tilde{b}_a}^2), \\ H_b &= -\frac{2\alpha_s}{3\pi} \frac{G_{ab}^*}{m_b \tan \beta} [m_t R_{2b}^{(t)} R_{2a}^{(b)*} (C_{11} - C_{12}) + m_b R_{1b}^{(t)} R_{1a}^{(b)*} C_{12} \\ &\quad + M_{\tilde{g}} R_{1b}^{(t)} R_{2a}^{(b)*} C_0] (m_t^2, M_{H^+}^2, m_b^2, M_{\tilde{g}}^2, M_{\tilde{t}_b}^2, M_{\tilde{b}_a}^2), \end{aligned} \quad (17)$$

$R^{(q)}$ are given in eq.(7) and we have used G_{ab} to parametrize the $H^+ \tilde{b}_a \tilde{t}_b$ coupling. The expression for G_{ab} is given in the Appendix A.

Finally, the contributions from the SUSY-QCD sector to the quark self-energies are:

$$\begin{aligned} \Sigma_L^q(p^2) &= -\frac{2\alpha_s}{3\pi} |R_{1a}^{(q)}|^2 B_1(p^2, M_{\tilde{g}}^2, M_{\tilde{q}_a}^2), \\ \Sigma_R^q(p^2) &= -\frac{2\alpha_s}{3\pi} |R_{2a}^{(q)}|^2 B_1(p^2, M_{\tilde{g}}^2, M_{\tilde{q}_a}^2), \\ \Sigma_S^q(p^2) &= -\frac{2\alpha_s}{3\pi} \frac{m_{\tilde{g}}}{m_q} \text{Re}(R_{1a}^{(q)} R_{2a}^{(q)*}) B_0(p^2, M_{\tilde{g}}^2, M_{\tilde{q}_a}^2). \end{aligned} \quad (18)$$

We have decomposed the quark self-energy according to

$$\Sigma^f(p) = \Sigma_L^f(p^2) \not{P}_L + \Sigma_R^f(p^2) \not{P}_R + m_f \Sigma_S^f(p^2), \quad (19)$$

and used the notation $\Sigma'(p) \equiv \partial\Sigma(p)/\partial p^2$.

Our notation for the one-loop integrals that appear in the above formulae, B_0 , B'_0 , B_1 , B'_1 , C_0 , C_{11} and C_{12} , is defined in the Appendix B. We have checked that these results are in agreement with the calculation of [12, 13].

4 Large SUSY mass limit in the MSSM

Here we study the effect of heavy SUSY particles in the SUSY-QCD correction to $H^+ \rightarrow t\bar{b}$. We derive approximate expansions for this correction in the limit of large SUSY mass parameters as compared to the electroweak scale, M_{EW} , which corresponds to a SUSY spectrum heavier than the Standard Model one.

To define our expansion parameters, we consider all the soft-SUSY-breaking mass parameters and the μ parameter to be of the same order (collectively denoted by M_{SUSY}) and much heavier than the electroweak scale. That is,

$$M_{SUSY} \sim M_{\tilde{Q}} \sim M_{\tilde{U}} \sim M_{\tilde{D}} \sim M_{\tilde{g}} \sim \mu \sim A_t \sim A_b \gg M_{EW}, \quad (20)$$

where all these parameters are defined in Section 2. Notice that, with $M_{SUSY} \sim \mathcal{O}(1TeV)$, this choice will lead to a plausible situation where all the SUSY particles in the SUSY-QCD sector are much heavier than their SM partners.³

We compute the expansions of the SUSY-QCD correction to the partial decay width $\Gamma(H^+ \rightarrow t\bar{b})$ in inverse powers of the SUSY mass parameters, up to order M_{EW}^2/M_{SUSY}^2 , considering that all M_{H^+} , M_Z , M_W , m_t and m_b are of order M_{EW} . In this section we present the leading terms of these expansions while the complete expressions are shown in the Appendix C.

We consider here two possible extreme configurations of the squarks mass-squared matrices corresponding to maximal and near-zero mixing respectively. This situation leads us to four extreme cases that will be considered in the present work:

- Maximal mixing in the sbottom and stop sectors ($\theta_{\tilde{b}} \sim \pm 45^\circ$, $\theta_{\tilde{t}} \sim \pm 45^\circ$),
- Near zero mixing in the sbottom and stop sectors ($\theta_{\tilde{b}} \sim 0^\circ$, $\theta_{\tilde{t}} \sim 0^\circ$),
- Maximal mixing in the sbottom sector and near zero mixing in the stop sector ($\theta_{\tilde{b}} \sim \pm 45^\circ$, $\theta_{\tilde{t}} \sim 0^\circ$),
- Near zero mixing in the sbottom sector and maximal mixing in the stop sector ($\theta_{\tilde{b}} \sim 0^\circ$, $\theta_{\tilde{t}} \sim \pm 45^\circ$).

³Notice that our choice of large μ is not a necessary condition to get all the SUSY-QCD particles heavy but it is needed in order to get all the gauginos heavy in the electroweak sector.

Maximal mixing ($\theta_{\tilde{q}} \sim \pm 45^\circ$) arises when the splitting between the diagonal elements of the mass-squared matrix is small compared to the off-diagonal elements, that is $|M_L^2 - M_R^2| \ll m_t|X_t|$ in the stop sector or $|M_L'^2 - M_R'^2| \ll m_b|X_b|$ in the sbottom sector. This situation leads to small mass splitting between the two squarks compared with the masses themselves, namely, $|M_{\tilde{q}_1}^2 - M_{\tilde{q}_2}^2| \ll |M_{\tilde{q}_1}^2 + M_{\tilde{q}_2}^2|$. In order to define properly the large SUSY mass expansions in powers of a small expansion parameter, we notice that all mass scales should be referred either to M_{EW} or to M_{SUSY} . Thus, the counting in this maximal case goes as follows: $m_q X_q$ is of order $M_{EW} M_{SUSY}$, while the splitting between the diagonal mass-squared terms is of order M_{EW}^2 , so that the mass-squared eigenvalues can be written as:

$$M_{\tilde{t}_{1,2}}^2 \simeq M_S^2 \pm \Delta_t^2 \text{ or/and } M_{\tilde{b}_{1,2}}^2 \simeq \tilde{M}_S^2 \pm \Delta_b^2, \quad (21)$$

where we have defined:

$$M_S^2 = \frac{1}{2}(M_{\tilde{t}_1}^2 + M_{\tilde{t}_2}^2), \quad \tilde{M}_S^2 = \frac{1}{2}(M_{\tilde{b}_1}^2 + M_{\tilde{b}_2}^2), \quad (22)$$

$$\begin{aligned} \Delta_t^2 &= m_t|X_t| \left[1 + \frac{(M_L^2 - M_R^2)^2}{8m_t^2 X_t^2} \right], \\ \Delta_b^2 &= m_b|X_b| \left[1 + \frac{(M_L'^2 - M_R'^2)^2}{8m_b^2 X_b^2} \right], \end{aligned} \quad (23)$$

and M_L , M_R , M'_L and M'_R are defined in eqs. (5). Here M_S^2 and \tilde{M}_S^2 are of order M_{SUSY}^2 while Δ_t^2 and Δ_b^2 are of order $M_{EW} M_{SUSY}$. The quantities $\frac{M_L^2 - M_R^2}{m_t X_t}$ and $\frac{M_L'^2 - M_R'^2}{m_b X_b}$ are therefore small and of order M_{EW}/M_{SUSY} . Expanding the expressions for the mixing angle in terms of these small parameters, we obtain for $\theta_{\tilde{q}} \simeq 45^\circ$:

$$\begin{aligned} \cos 2\theta_{\tilde{t}} &\simeq \frac{M_L^2 - M_R^2}{2m_t X_t}, \quad \cos 2\theta_{\tilde{b}} \simeq \frac{M_L'^2 - M_R'^2}{2m_b X_b}, \\ \sin 2\theta_{\tilde{t}} &\simeq \sigma_{X_t} \left[1 - \frac{(M_L^2 - M_R^2)^2}{8m_t^2 X_t^2} \right], \\ \sin 2\theta_{\tilde{b}} &\simeq \sigma_{X_b} \left[1 - \frac{(M_L'^2 - M_R'^2)^2}{8m_b^2 X_b^2} \right]. \end{aligned} \quad (24)$$

where $\sigma_{X_q} \equiv \text{sgn}(X_q)$ with $q = t, b$.

Near-zero mixing ($\theta_{\tilde{q}} \simeq 0^\circ$) arises when the splitting between the diagonal elements of the mass-squared matrix is large compared to the off-diagonal elements, that is $|M_L^2 - M_R^2| \gg m_t|X_t|$ in the stop sector or $|M_L'^2 - M_R'^2| \gg m_b|X_b|$ in the sbottom sector. This is the case usually considered in the literature, because M_L (M'_L) and M_R (M'_R) depend on two different (and a priori independent) soft-SUSY-breaking parameters $M_{\tilde{Q}}$ and $M_{\tilde{U}}$ ($M_{\tilde{D}}$), respectively. The counting in terms of M_{EW} and M_{SUSY} is such that $(M_L^2 -$

M_R^2) (or $(M_L'^2 - M_R'^2)$) is of order M_{SUSY}^2 while $m_q X_q$ is of order $M_{EW} M_{SUSY}$. The mass splitting between the two squarks will be of the same order as the masses themselves, that is $|M_{\tilde{q}_1}^2 - M_{\tilde{q}_2}^2| \sim \mathcal{O}(|M_{\tilde{q}_1}^2 + M_{\tilde{q}_2}^2|) \sim \mathcal{O}(M_{SUSY}^2)$. As in the maximal mixing case, all mass scales should be referred to M_{EW} or to M_{SUSY} in order to define the expansion parameters. In this case we write our results in terms of the physical stop and sbottom masses and the mixing angles which are given by:

$$\sin 2\theta_{\tilde{q}} = \frac{2m_q X_q}{M_{\tilde{q}_1}^2 - M_{\tilde{q}_2}^2}, \quad (25)$$

$$\cos 2\theta_{\tilde{q}} \simeq 1 - \frac{2m_q^2 X_q^2}{(M_{\tilde{q}_1}^2 - M_{\tilde{q}_2}^2)^2}. \quad (26)$$

4.1 The decoupling regime in $H^+ \rightarrow t\bar{b}$ decay

Now we study, both analytically and numerically, the SUSY-QCD correction to $\Gamma(H^+ \rightarrow t\bar{b})$ in the large SUSY mass parameters limit. We consider here all the possible extreme configurations of the squarks mass-squared matrix, namely the four cases mentioned above. We will study also the individual decoupling of the various SUSY particles, that is, decoupling of gluinos and squarks separately. In this analysis we use the leading term of our expansions for Δ_{SQCD} while the complete expressions, up to order M_{EW}^2/M_{SUSY}^2 , are given in the Appendix C.

First we consider maximal mixing in both the stop and sbottom sectors. In this case, and in the large SUSY mass parameters limit defined in eq. (20), we obtain $M_L^2 \simeq M_R^2$ and $M_L'^2 \simeq M_R'^2$, up to corrections of order M_{EW}^2/M_{SUSY}^2 . Since M_L and M_L' are determined by the same soft-SUSY breaking term $M_{\tilde{Q}}$, we also have $M_L^2 \simeq M_L'^2$. From these relations and from eq. (23) we obtain $M_S^2 \simeq \tilde{M}_S^2$, up to corrections of order M_{EW}^2/M_{SUSY}^2 .

Taking this into account we expand the SUSY-QCD contributions to the $H^+ \rightarrow t\bar{b}$ partial width and we find:

$$\Delta_{SQCD} = -\frac{\alpha_s}{3\pi} \frac{M_{\tilde{g}} \mu}{M_S^2} (\tan \beta + \cot \beta) f_1(R) + \mathcal{O}(M_{EW}^2/M_{SUSY}^2) \quad (27)$$

where $R = M_{\tilde{g}}/M_S$. The expression for $f_1(R)$, which arises from the expansions of the loop integrals, is given in Appendix B and it is normalized so that $f_1(1) = 1$. The complete formula for Δ_{SQCD} , including the $\mathcal{O}(\frac{M_{EW}^2}{M_{SUSY}^2})$ terms, is given in Appendix C.

We can see from eq. (27) that, taking all SUSY mass parameters arbitrarily large and of the same order, Δ_{SQCD} leads to a non-zero value. That is, the SUSY-QCD correction *do not decouple* in the large SUSY mass parameters regime. This can be seen clearly, for instance, in the simplest case of equal mass scales, $\mu = M_{\tilde{g}} = M_S$, where $f_1(R) = 1$, leading to

$$\Delta_{SQCD} = -\frac{\alpha_s}{3\pi} (\tan \beta + \cot \beta) + \mathcal{O}(M_{EW}^2/M_{SUSY}^2), \quad (28)$$

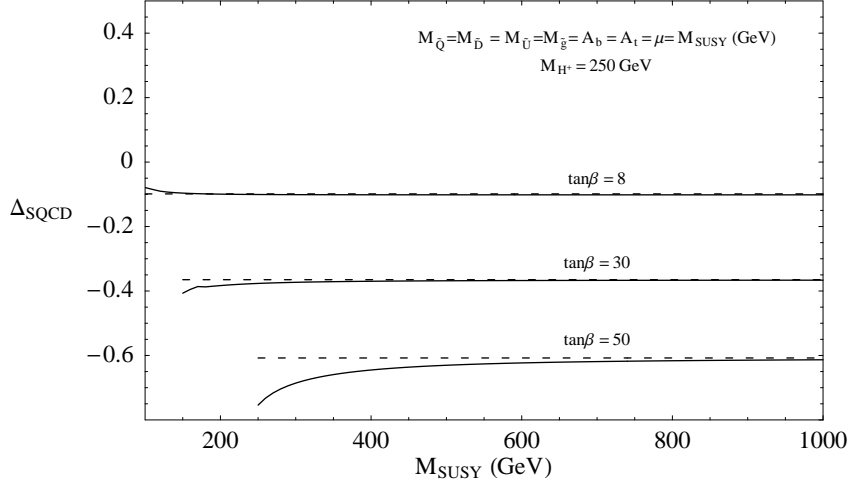


Figure 2: *Non-decoupling behavior of Δ_{SQCD} with $M_{\tilde{Q}} = M_{\tilde{U}} = M_{\tilde{D}} = M_{\tilde{g}} = A_b = A_t = \mu = M_{SUSY}$ and for different values of $\tan\beta$. Exact one-loop result (solid lines) and the expansion given in eq. (27) (dashed lines) are plotted for comparison.*

which shows that the first term in the large M_{SUSY} expansion is indeed of $\mathcal{O}(M_{EW}^0/M_{SUSY}^0)$. This leading contribution, when considered in the large $\tan\beta$ regime and expressed in terms of an effective coupling of H^+ to $b\bar{t}$ is in agreement with the previous results of refs. [20] that were obtained in the zero external momentum approximation by using an effective Lagrangian approach.

Notice also that this non-decoupling term is enhanced by a $\tan\beta$ factor and therefore a numerically large SUSY-QCD correction in the large $\tan\beta$ limit is expected. This non-decoupling behavior is shown numerically in Fig. 2. In this figure we plot the exact one-loop result (solid lines) and the leading term of the large SUSY mass expansion in eq. (27) (dashed lines) for $M_{\tilde{Q}} = M_{\tilde{U}} = M_{\tilde{D}} = M_{\tilde{g}} = A_b = A_t = \mu = M_{SUSY}$ and for different values of $\tan\beta$. For all the numerical analyses, in this work we fix $M_{H^+} = 250$ GeV. We can see in this figure that for large SUSY mass parameters (say $M_{SUSY} \geq 300$ GeV), Δ_{SQCD} tends to a non-zero value whose size is larger for larger $\tan\beta$ values. Indeed the correction can be quite large for large $\tan\beta$ even for quite heavy SUSY particles. For example for $M_{SUSY} = 1$ TeV and $\tan\beta = 30$ we get $\Delta_{SQCD} \simeq -35\%$, and it grows linearly with $\tan\beta$.

From the numerical comparison in Fig. 2 between the exact and our approximate result of eq. (27), we can conclude that this expansion, with just the leading term, is a good approximation for large enough SUSY mass parameters. It is clear also that as $\tan\beta$ grows the agreement between the exact and approximate results becomes worse at low M_{SUSY} . However, we can conclude that the agreement is still quite good even for $\tan\beta$ as large as

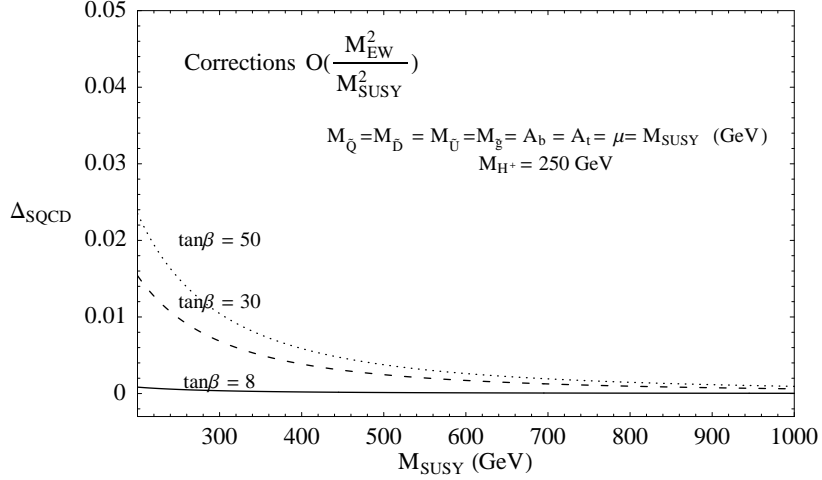


Figure 3: *Behaviour of the contributions to Δ_{SQCD} of $\mathcal{O}(M_{EW}^2/M_{SUSY}^2)$ for $M_{\tilde{Q}} = M_{\tilde{U}} = M_{\tilde{D}} = M_{\tilde{g}} = A_b = A_t = \mu = M_{SUSY}$ and for different values of $\tan\beta$.*

50 whenever $M_{SUSY} \geq 300$ GeV.

For lower values of M_{SUSY} the next to leading corrections, i.e. the corrections of order M_{EW}^2/M_{SUSY}^2 which are given in Appendix C, begin to be important. We have estimated the size of these corrections for several choices of the parameter space and we have found that they are of order of a few percent. Besides, they grow with the μ parameter and with $\tan\beta$ and are almost independent of the value for the trilinear couplings, $A_{t,b}$. We show in Fig. 3 the numerical results for the particular case $M_{\tilde{Q}} = M_{\tilde{U}} = M_{\tilde{D}} = M_{\tilde{g}} = A_b = A_t = \mu = M_{SUSY}$ and for several values of $\tan\beta$. We can see clearly that their size is always small as compared to the leading non-decoupling term. For other choices of the parameters similar results are found.

In eq. (27) we can see that, in the approximation of large SUSY mass parameters, changing the sign of $M_{\tilde{g}}\mu$ simply flips the sign of the SUSY-QCD correction. In most of this work, and for the numerical analysis, a positive sign for $M_{\tilde{g}}\mu$ has been chosen.

In Fig. 4 we show the exact SUSY-QCD correction as a function of μ (left) and as a function of $\tan\beta$ (right). In the left panel we plot Δ_{SQCD} for different values of $\tan\beta$ and fixing $M_{\tilde{Q}} = M_{\tilde{U}} = M_{\tilde{D}} = M_{\tilde{g}} = A_b = A_t = 1$ TeV. We see that the size of the correction grows linearly with μ and notice that by changing the sign of μ the sign of the correction changes. In the right panel we plot the SUSY-QCD correction as a function of $\tan\beta$ for the choice $M_{\tilde{Q}} = M_{\tilde{U}} = M_{\tilde{D}} = M_{\tilde{g}} = A_b = A_t = \mu = M_{SUSY}$ and for different values of M_{SUSY} . We see explicitly that for large M_{SUSY} the size of the correction grows linearly with $\tan\beta$.

In comparing the various contributions to Δ_{SQCD} we find that the domi-

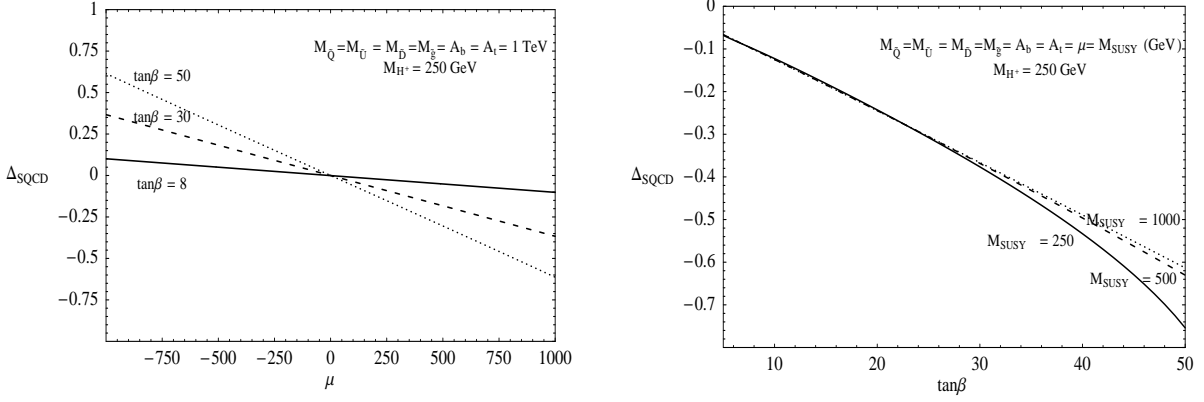


Figure 4: Δ_{SQCD} as a function of μ and $\tan\beta$.

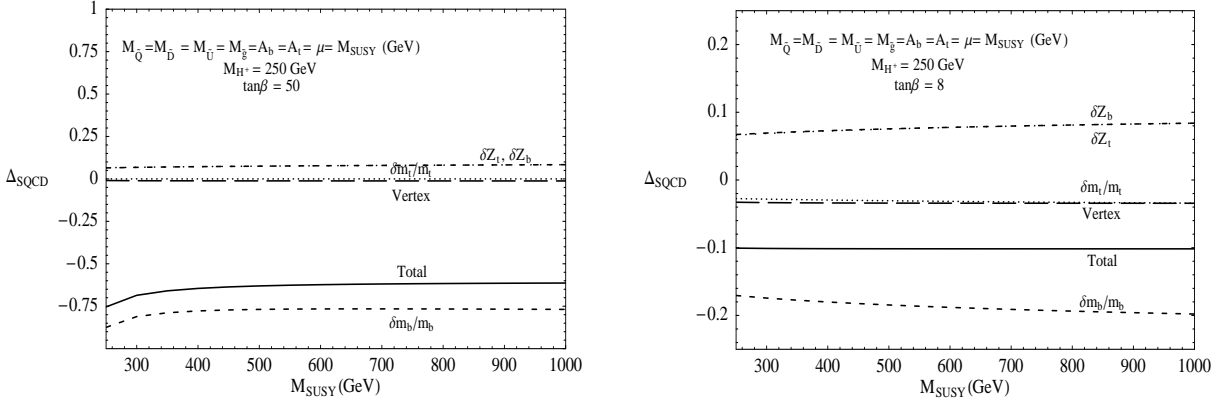


Figure 5: Comparison of contribution coming from $\delta m_b/m_b$ (lower dashed line), δZ_b (upper dashed line), $\delta m_t/m_t$ (lower dotted line), δZ_t (upper dotted line) and vertex contributions (long-dashed line) for different values of $\tan\beta$. Total correction is also plotted (solid line).

nant contributions come from the renormalization of the bottom-quark mass and wavefunction. In Fig. 5 the total SUSY-QCD correction (Total), the contributions from the bottom-quark mass ($\delta m_b/m_b$) and wavefunction (δZ_b) counterterms, the contributions from the top-quark mass ($\delta m_t/m_t$) and wavefunction (δZ_t) counterterms and the vertex contributions (Vertex) are shown separately. We can see that the contributions from $\delta m_b/m_b + \delta Z_b$ dominate Δ_{SQCD} at large $\tan\beta$.

For the three cases left, near-zero stop and sbottom mixing, near-zero stop-maximal sbottom mixing and near-zero sbottom-maximal stop mixing, we have found a leading term in Δ_{SQCD} that is very similar to the one in eq. (27). The general expression is:

$$\Delta_{SQCD} = -\frac{\alpha_s}{3\pi} \frac{M_{\tilde{g}}\mu}{\hat{M}_S^2} (\tan\beta + \cot\beta) F_{mix} + \mathcal{O}(M_{EW}^2/M_{SUSY}^2), \quad (29)$$

where \hat{M}_S^2 and F_{mix} depend on the case:

- Near-zero stop and sbottom mixing:

$$\hat{M}_S^2 = M_{\tilde{t}_1}^2 \text{ and } F_{mix} = f_1(R_1, R_2) \text{ where } R_i = M_{\tilde{g}}/M_{\tilde{q}_i} \text{ and } M_{\tilde{t}_i} \simeq M_{\tilde{b}_i} \simeq M_{\tilde{q}_i}, i=1,2 .$$

- Near-zero stop-maximal sbottom mixing:

$$\hat{M}_S^2 = \tilde{M}_S^2 \text{ and } F_{mix} = \frac{U_t}{D} f_1(R_b, R_{t_2}) + \frac{U_b}{D} f_1(R_b) \text{ where } R_{t_2} = M_{\tilde{g}}/M_{\tilde{t}_2} \text{ and } R_b = M_{\tilde{g}}/\tilde{M}_S .$$

- Near-zero sbottom-maximal stop mixing:

$$\hat{M}_S^2 = M_S^2 \text{ and } F_{mix} = \frac{U_t}{D} f_1(R_t) + \frac{U_b}{D} f_1(R_t, R_{b_2}) \text{ where } R_{b_2} = M_{\tilde{g}}/M_{\tilde{b}_2} \text{ and } R_t = M_{\tilde{g}}/M_S .$$

The functions $f_1(R)$ and $f_1(R_1, R_2)$ are defined in the Appendix B and are normalized such that $f_1(1, 1) = f_1(1) = 1$. M_S and \tilde{M}_S are defined in eq. (22). The corrections in eq. (29) of $\mathcal{O}(\frac{M_{EW}^2}{M_{SUSY}^2})$ are given explicitly in Appendix C.

In eq. (29) we see that the non-decoupling contribution to Δ_{SQCD} appears in all the cases so that we can conclude that the SUSY-QCD corrections *do not decouple* in the large SUSY mass parameters regime. We also see that Δ_{SQCD} grows again linearly with $\tan \beta$, thus we expect large corrections in the large $\tan \beta$ limit for all the cases.

Now we study the decoupling behaviour of the SUSY-QCD corrections as individual SUSY particles become heavier than a reference SUSY mass scale so that there is a hierarchy among the various SUSY particle masses. We will consider two cases: large gluino mass with maximal mixing in stop and sbottom sectors and large squark masses (stop and sbottom) with maximal mixing in both sectors.

First, we examine the case of a very heavy gluino compared with the rest of the SUSY spectrum and with maximal mixing in sbottom and stop sectors. In this case $M_{\tilde{g}} \gg M_{SUSY} \gg M_{EW}$. We evaluate the SUSY-QCD correction when the gluino mass is taken very large while the rest of the SUSY mass parameters remain fixed to a reference value of the order of M_{SUSY} (larger than the electroweak scale). Our result for Δ_{SQCD} is:

$$\Delta_{SQCD} = \frac{2\alpha_s}{3\pi} (\tan \beta + \cot \beta) \left(1 - \log \frac{M_{\tilde{g}}^2}{M_S^2} \right) \frac{\mu}{M_{\tilde{g}}} + \mathcal{O}\left(\frac{M_{EW}^2}{M_{SUSY} M_{\tilde{g}}}\right). \quad (30)$$

In eq. (30) we see that the SUSY-QCD correction *decouples* when we take the large gluino mass limit while the rest of the SUSY mass parameters (μ and M_S) remain fixed at some scale of the order M_{SUSY} . We also notice that this decoupling is very slow: Δ_{SQCD} falls off when increasing $M_{\tilde{g}}$ as $\frac{\log M_{\tilde{g}}}{M_{\tilde{g}}}$. We see again that the correction is enhanced by a $\tan \beta$ factor, so we expect large SUSY-QCD corrections in the large $\tan \beta$ limit. In Fig. 6 we plot the

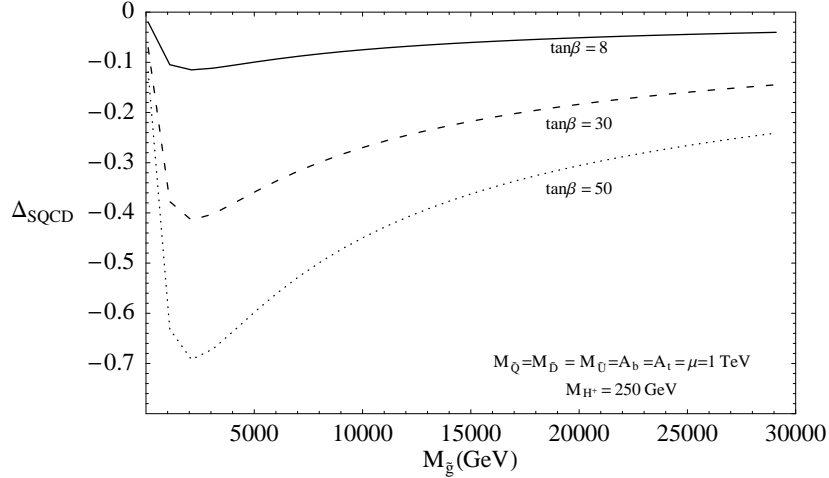


Figure 6: *Behaviour of Δ_{SQCD} in the large $M_{\tilde{g}}$ limit with fixed $M_{\tilde{Q}} = M_{\tilde{U}} = M_{\tilde{D}} = A_b = A_t = \mu = 1$ TeV and for different values of $\tan \beta$.*

exact result for Δ_{SQCD} as a function of $M_{\tilde{g}}$ and keeping the other SUSY mass parameters fixed at 1 TeV. We can see the slow decoupling with the gluino mass and the numerically large correction even for very heavy gluino; for example if $M_{\tilde{g}} = 2$ TeV and $\tan \beta = 30$ we find $\Delta_{SQCD} \simeq -40\%$. Notice that the size can be so large that the validity of the perturbative expansion can be questionable. We refer the reader to refs. [20] where this subject is studied in more detail and some techniques of resummation for a better convergence of the series are proposed.

Next we analyze the large squark (stop and sbottom) mass limit with maximal mixing in both sectors. We consider the case with $M_S = \tilde{M}_S \gg M_{\tilde{g}} = A_t = A_b = \mu \gg M_{EW}$. If we expand the eq. (27) in the limit of large squark masses we obtain:

$$\Delta_{SQCD} = -\frac{2\alpha_s}{3\pi} \frac{M_{\tilde{g}}\mu}{M_S^2} (\tan \beta + \cot \beta) + \mathcal{O}(M_{EW}^2/M_{SUSY}^2). \quad (31)$$

As we can see in eq. (31), the correction *decouples* in the large squark mass limit if the rest of the SUSY mass parameters ($M_{\tilde{g}}$ and μ) remain fixed at some scale larger than the electroweak scale. This decoupling is faster than the previous case since Δ_{SQCD} is proportional to the inverse of M_S^2 , that is the scale of the squark masses. We also see that the correction is enhanced by a $\tan \beta$ factor. Finally we have also confirmed this decoupling behaviour of squarks numerically, as can be seen in Fig. 7, where the explicit result of Δ_{SQCD} , as a function of $M_{SUSY} = M_{\tilde{Q}} = M_{\tilde{D}} = M_{\tilde{U}}$, is shown for several values of $\tan \beta$.

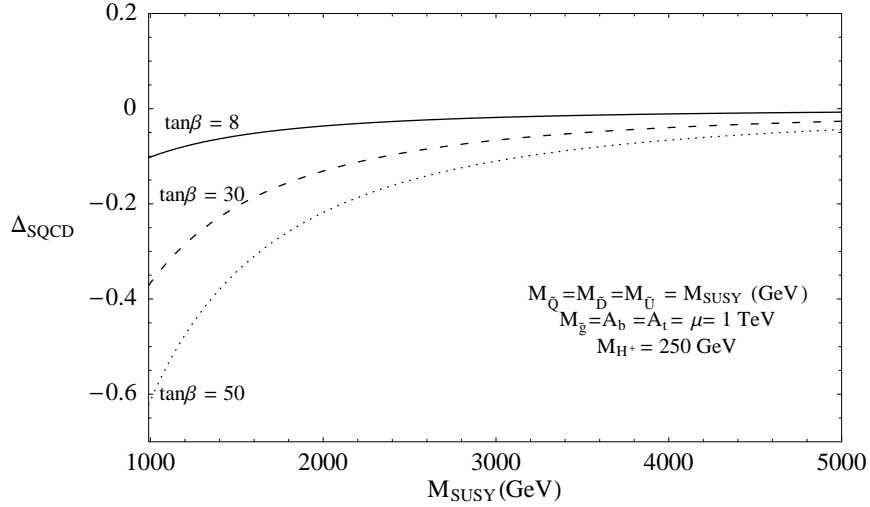


Figure 7: Behaviour of Δ_{SQCD} in the large squark masses limit with fixed $M_{\tilde{g}} = A_b = A_t = \mu = 1$ TeV and for different values of $\tan\beta$.

5 Conclusions

In this work we have looked for indirect SUSY signals through the effect of radiative corrections to the $H^+ \rightarrow t\bar{b}$ decay in the limit of large SUSY masses. We have focused on the well known large SUSY-QCD corrections to the $\Gamma(H^+ \rightarrow t\bar{b})$ partial decay width. We have studied in detail the one-loop SUSY-QCD corrections to $\Gamma(H^+ \rightarrow t\bar{b})$ when the SUSY particles are heavier than the SM ones. In order to understand analytically the behaviour of these corrections in the large SUSY mass limit, we have performed expansions of the one-loop partial width that are valid for large values of the SUSY mass parameters compared to the electroweak scale and for various choices of the mixing in the squarks sector.

We have shown that for large SUSY mass parameters and all of the same order, the SUSY-QCD radiative corrections do not decouple in the $H^+ \rightarrow t\bar{b}$ decay. In other words, if there are heavy squarks and gluinos, with masses of the same order and much larger than the SM particles, they will produce a non-vanishing contribution, via SUSY-QCD radiative corrections, to the potentially measurable partial width $\Gamma(H^+ \rightarrow t\bar{b})$. We would like to remind that the conclusion about decoupling or non-decoupling of SUSY particles in the MSSM is not immediate, since the decoupling theorem does not apply to this case, because the MSSM is a theory involving chiral fermions and the spontaneous breaking of the electroweak symmetry. Therefore, the SUSY decoupling behaviour must be explored case by case. In this direction it has been shown by an explicit calculation [9] that there is decoupling of heavy SUSY particles in observables with external electroweak gauge bosons.

We interpret the *non-decoupling* effect found in the present work (as well

as the one found in [10]) as follows. If we start from the full MSSM as the theory valid at large energies and integrate out the heavy SUSY spectrum, we are left with a low energy theory, valid at the electroweak scale, which contains the Standard Model particles plus two full Higgs doublets. The interactions of this effective low energy theory are a priori unknown, but they can be derived by explicit integration of the heavy SUSY particles [22]. The Higgs-fermion-fermion interactions of the MSSM are like those of a two Higgs doublet model (2HDM) of type II. In a 2HDM of type II there are some restrictions on the allowed couplings, which in the MSSM case are a consequence of supersymmetry. Once the heavy SUSY particles are integrated out, new low energy effective Higgs-fermion-fermion interactions with no restrictions anymore can be generated since SUSY is a (softly) broken symmetry. Indeed, one expects to find the most general 2HDM of type III, where both Higgs doublets can couple to both u and d type fermions. However, to show this one must perform explicitly the computation and find out the specific values of the generated effective couplings [22].

We also emphasize here that these non-decoupling SUSY-QCD corrections could give us an indirect signal of supersymmetry at present and future colliders even for a very heavy SUSY spectrum at the TeV scale. In particular they can provide some clues in the indirect search of a heavy SUSY spectrum in the LHC [23] and next linear colliders.

We have also examined in this work some special cases in which there is a hierarchy among the SUSY mass parameters. In the case of maximal squark mixing with $M_S = \tilde{M}_S$ large and the other SUSY mass parameters of order a common mass scale M (chosen such that $M_{EW} \ll M \ll M_S$), the SUSY-QCD corrections decouple like M^2/M_S^2 . In addition, we have examined the case of a large gluino mass with the other SUSY mass parameters of order a common mass scale M (chosen such that $M_{EW} \ll M \ll M_{\tilde{g}}$). In this case we have found that the SUSY-QCD corrections decouple more slowly, like $(M/M_{\tilde{g}}) \log(M_{\tilde{g}}^2/M_S^2)$. This indicates that sizeable indirect signals from gluinos as heavy as several TeV can be obtained in the $H^+ \rightarrow t\bar{b}$ decay.

Finally we have seen that, in all cases, the corrections are enhanced by a $\tan \beta$ factor and therefore large SUSY-QCD contributions to the $H^+ \rightarrow t\bar{b}$ decay are expected for large values of $\tan \beta$, even for a very heavy SUSY spectrum.

Acknowledgments

This work has been supported in part by the Spanish Ministerio de Ciencia y Tecnología under project CICYT FPA 2000-0980. S.P. was partially supported by the Ramon Areces Foundation at the Karlsruhe University. S.P. wishes to thank W. Hollik for reading the manuscript.

Appendices

A $H^\pm \tilde{t} \tilde{b}$ interaction Lagrangian

The $H^+ \tilde{t}^* \tilde{b}$ and $H^- \tilde{t} \tilde{b}^*$ interaction terms are given by the following interaction Lagrangian [1]:

$$\mathcal{L}_{H^\pm \tilde{t} \tilde{b}} = -\frac{g}{\sqrt{2}M_W} H^\pm \left(g_{LL} \tilde{b}_L^* \tilde{t}_L + g_{RR} \tilde{b}_R^* \tilde{t}_R + g_{LR} \tilde{b}_R^* \tilde{t}_L + g_{RL} \tilde{b}_L^* \tilde{t}_R \right) + h.c. , \quad (\text{A.1})$$

where:

$$\begin{aligned} g_{LL} &= M_W^2 \sin 2\beta - (m_t^2 \cot \beta + m_b^2 \tan \beta) , \\ g_{RR} &= -m_t m_b (\tan \beta + \cot \beta) , \\ g_{LR} &= -m_b (\mu + A_b \tan \beta) , \\ g_{RL} &= -m_t (\mu + A_t \cot \beta) . \end{aligned} \quad (\text{A.2})$$

In the mass eigenstate basis for the squarks, these interaction terms can be parametrized as follows:

$$\mathcal{L}_{H^\pm \tilde{t} \tilde{b}} = -\frac{g}{\sqrt{2}M_W} H^\pm G_{ab} \tilde{b}_a^* \tilde{t}_b + h.c. \quad (\text{A.3})$$

where

$$G_{ab} = R_{1a}^{(b)*} R_{1b}^{(t)} g_{LL} + R_{2a}^{(b)*} R_{2b}^{(t)} g_{RR} + R_{2a}^{(b)*} R_{1b}^{(t)} g_{LR} + R_{1a}^{(b)*} R_{2b}^{(t)} g_{RL} . \quad (\text{A.4})$$

B Large mass expansion of loop integrals

Here we define the notation for the two- and three-point integrals that appear in eqs. (17) and (18) and give formulae for their expansions in inverse powers of the SUSY mass parameters.

We follow the definitions and conventions of [21]. The integrals are performed in $D = 4 - \epsilon$ dimensions and the divergent contributions are regularized by $\Delta = \frac{2}{\epsilon} - \gamma_E + \log(4\pi)$, with the corresponding inclusion of the energy scale given here by μ_0 .

The two-point integrals are given by:

$$\mu_0^{4-D} \int \frac{d^D k}{(2\pi)^D} \frac{\{1; k^\mu\}}{[k^2 - m_1^2][(k+q)^2 - m_2^2]} = \frac{i}{16\pi^2} \{B_0; q^\mu B_1\} (q^2; m_1^2, m_2^2) . \quad (\text{B.5})$$

The derivatives of the two-point functions are defined as follows:

$$B'_{0,1}(p^2; m_1^2, m_2^2) = \left. \frac{\partial}{\partial q^2} B_{0,1}(q^2; m_1^2, m_2^2) \right|_{q^2=p^2} . \quad (\text{B.6})$$

Finally, the three-point integrals are given by:

$$\begin{aligned} & \mu_0^{4-D} \int \frac{d^D k}{(2\pi)^D} \frac{\{1; k^\mu\}}{[k^2 - m_1^2][(k + p_1)^2 - m_2^2][(k + p_1 + p_2)^2 - m_3^2]} \\ &= \frac{i}{16\pi^2} \{C_0; p_1^\mu C_{11} + p_2^\mu C_{12}\} (p_1^2, p_2^2, p^2; m_1^2, m_2^2, m_3^2), \end{aligned} \quad (\text{B.7})$$

where $p = -p_1 - p_2$.

We next give the large M_{SUSY} expansions of the one-loop integrals in the four different cases that we have mentioned in section 4.

B.1 Maximal sbottom and stop mixing

The results of the large M_{SUSY} expansions of the loop integrals are as follows:

$$\begin{aligned} & C_0(m_t^2, M_{H^+}^2, m_b^2; M_{\tilde{g}}^2, M_{\tilde{t}_i}^2, M_{\tilde{b}_j}^2) \\ & \simeq -\frac{1}{2M_S^2} f_1(R_t, R_b) - \frac{m_t^2}{24M_S^4} f_2(R_t, R_b) - \frac{M_{H^+}^2}{24M_S^4} f_3(R_t, R_b) - \frac{m_b^2}{24M_S^4} f_4(R_t, R_b) \\ & \quad - (-1)^i \frac{\Delta_t^2}{6M_S^4} f_5(R_t, R_b) - (-1)^j \frac{\Delta_b^2}{6M_S^4} f_6(R_t, R_b) \\ & \quad - \frac{\Delta_t^4}{12M_S^6} f_7(R_t, R_b) - \frac{\Delta_b^4}{12M_S^6} f_8(R_t, R_b) - (-1)^{i+j} \frac{\Delta_t^2 \Delta_b^2}{12M_S^6} f_9(R_t, R_b), \\ & C_{11}(m_t^2, M_{H^+}^2, m_b^2; M_{\tilde{g}}^2, M_{\tilde{t}_i}^2, M_{\tilde{b}_j}^2) \\ & \simeq \frac{1}{3M_S^2} f_{10}(R_t, R_b) + (-1)^i \frac{\Delta_t^2}{8M_S^4} f_{11}(R_t, R_b) + (-1)^j \frac{\Delta_b^2}{8M_S^4} f_{12}(R_t, R_b), \\ & C_{12}(m_t^2, M_{H^+}^2, m_b^2; M_{\tilde{g}}^2, M_{\tilde{t}_i}^2, M_{\tilde{b}_j}^2) \\ & \simeq \frac{1}{6M_S^2} f_{13}(R_t, R_b) + (-1)^i \frac{\Delta_t^2}{24M_S^4} f_{14}(R_t, R_b) + (-1)^j \frac{\Delta_b^2}{12M_S^4} f_{15}(R_t, R_b), \\ & B_0(m_q^2; M_{\tilde{q}_i}^2, M_{\tilde{g}}^2) \simeq \Delta - \ln \frac{M_{\tilde{g}}^2}{R_q^2 \mu_0^2} + g_1(R_q) + (-1)^i \frac{\Delta_q^2}{2M_S^2} f_1(R_q) \\ & \quad + \frac{m_q^2}{6M_S^2} f_2(R_q) + \frac{\Delta_q^4}{6M_S^4} f_2(R_q) + (-1)^i \frac{m_q^2 \Delta_q^2}{12M_S^4} (2f_3 - f_4)(R_q), \\ & B_1(m_q^2; M_{\tilde{q}_i}^2, M_{\tilde{g}}^2) \simeq -\frac{1}{2}(\Delta - \ln \frac{M_{\tilde{g}}^2}{R_q^2 \mu_0^2}) + g_2(R_q) - (-1)^i \frac{\Delta_q^2}{6M_S^2} f_2(R_q) \\ & \quad - \frac{m_q^2}{12M_S^2} f_3(R_q) - \frac{\Delta_q^4}{24M_S^4} (2f_3 - f_4)(R_q). \end{aligned} \quad (\text{B.8})$$

Where M_S^2 and Δ^2 are defined in eq. (23) and the functions f_i and g_i are given in terms of the ratios $R_t \equiv M_{\tilde{g}}/M_S$ and $R_b \equiv M_{\tilde{g}}/\tilde{M}_S$ as follows:

$$f_1(R_1, R_2) = -\frac{2R_2^2}{(1 - R_2^2)(1 - R_1^2)(R_2^2 - R_1^2)} \left[\ln \frac{R_1^2}{R_2^2} + R_1^2 \ln R_2^2 - R_2^2 \ln R_1^2 \right]$$

$$\begin{aligned}
f_2(R_1, R_2) = & \frac{12R_2^2}{(1-R_2^2)^2(1-R_1^2)^3(R_2^2-R_1^2)^2} [R_1^2 - R_1^6 - R_2^2 - 3R_1^2R_2^2 \\
& + R_1^6R_2^2 + 3R_1^4R_2^2 + 3R_2^4 - 3R_1^4R_2^4 - 2R_2^6 + 2R_1^2R_2^6 + 2R_1^4\ln R_1^2 \\
& + R_2^2\ln\frac{R_2^2}{R_1^2} - R_1^2R_2^2\ln R_1^2 - 3R_1^2R_2^2\ln R_2^2 - R_1^6R_2^2\ln R_2^2 - 4R_1^4R_2^2\ln R_1^2 \\
& + 2R_2^4\ln R_1^2 + 2R_1^2R_2^4\ln R_1^2 + 2R_1^4R_2^4\ln R_1^2 + 3R_1^4R_2^2\ln R_2^2 \\
& - R_2^6\ln R_1^2 - R_1^2R_2^6\ln R_1^2]
\end{aligned}$$

$$\begin{aligned}
f_3(R_1, R_2) = f_4(R_1, R_2) = & \frac{12R_2^4}{(1-R_2^2)^2(1-R_1^2)^2(R_1^2-R_2^2)^3} [3R_1^4 - 2R_1^2 \\
& - R_1^6 + 2R_2^2 + R_1^6R_2^2 - 3R_1^4R_2^2 - 3R_2^4 + 3R_2^4R_1^2 + R_2^6 - R_2^6R_1^2 \\
& + 2R_1^4\ln\frac{R_2^2}{R_1^2} - R_1^2\ln\frac{R_2^2}{R_1^2} - R_1^6\ln R_2^2 - R_2^2\ln\frac{R_2^2}{R_1^2} + 2R_2^2R_1^2\ln\frac{R_2^2}{R_1^2} \\
& - R_2^2R_1^4\ln R_2^2 + 4R_2^2R_1^4\ln R_1^2 + 2R_2^4\ln\frac{R_2^2}{R_1^2} - 4R_2^4R_1^2\ln R_2^2 \\
& + R_2^4R_1^2\ln R_1^2 + 2R_2^4R_1^4\ln\frac{R_2^2}{R_1^2} + R_2^6\ln R_1^2]
\end{aligned}$$

$$\begin{aligned}
f_5(R_1, R_2) = & -\frac{6R_2^2}{(1-R_2^2)(1-R_1^2)^2(R_1^2-R_2^2)^2} [-R_1^2 + R_1^4 + R_2^2 - R_1^4R_2^2 \\
& - R_2^4 + R_1^2R_2^4 - R_1^4\ln R_1^2 - R_2^2\ln\frac{R_2^2}{R_1^2} + 2R_2^2R_1^2\ln R_2^2 \\
& - R_2^2R_1^4\ln\frac{R_2^2}{R_1^2} - R_2^4\ln R_1^2]
\end{aligned}$$

$$\begin{aligned}
f_6(R_1, R_2) = & \frac{6R_2^4}{R_1^2(1-R_2^2)^2(1-R_1^2)(R_1^2-R_2^2)^2} [-R_1^2 + R_1^4 + R_2^2 - R_1^4R_2^2 \\
& - R_2^4 + R_1^2R_2^4 + R_1^4\ln R_2^2 - R_1^2\ln\frac{R_2^2}{R_1^2} - 2R_2^2R_1^2\ln R_1^2 \\
& - R_2^4R_1^2\ln\frac{R_2^2}{R_1^2} + R_2^4\ln R_2^2]
\end{aligned}$$

$$\begin{aligned}
f_7(R_1, R_2) = & \frac{6R_2^2}{(1-R_2^2)(1-R_1^2)^3(R_2^2-R_1^2)^3} [-R_1^4 + R_1^8 + 4R_2^2R_1^2 - 3R_2^2R_1^4 \\
& - R_2^2R_1^8 - 3R_2^4 + 3R_2^4R_1^4 + 3R_2^6 + R_2^6R_1^4 - 4R_2^6R_1^2 - 2R_1^6\ln R_1^2 \\
& + 6R_2^2R_1^4\ln R_1^2 - 6R_2^4R_1^2\ln R_2^2 + 2R_2^4\ln\frac{R_2^2}{R_1^2} + 6R_2^4R_1^4\ln\frac{R_2^2}{R_1^2} - 2R_2^4R_1^6\ln\frac{R_2^2}{R_1^2} \\
& + 2R_2^6\ln R_1^2]
\end{aligned}$$

$$\begin{aligned}
f_8(R_1, R_2) = & \frac{6R_2^6}{R_1^4(1-R_2^2)^3(1-R_1^2)(R_2^2-R_1^2)^3} [3R_1^4 - 3R_1^6 - 4R_2^2R_1^2 + 4R_2^2R_1^6 \\
& + 3R_2^4R_1^2 + R_2^4 - 3R_2^4R_1^4 - R_2^4R_1^6 - R_2^8 + R_2^8R_1^2 + 2R_1^4\ln\frac{R_2^2}{R_1^2} \\
& - 2R_1^6\ln R_2^2 + 6R_2^2R_1^4\ln R_1^2 - 6R_1^2R_2^4\ln R_2^2 + 6R_2^4R_1^4\ln\frac{R_2^2}{R_1^2}]
\end{aligned}$$

$$+ 2R_2^6 \ln R_2^2 - 2R_2^6 R_1^4 \ln \frac{R_2^2}{R_1^2} \Big]$$

$$\begin{aligned} f_9(R_1, R_2) = & \frac{12R_2^4}{R_1^2(1-R_2^2)^2(1-R_1^2)^2(R_1^2-R_2^2)^3} \left[R_2^6 + R_1^4 - R_1^6 + 3R_2^2 R_1^6 \right. \\ & - 2R_2^4 R_1^6 + 3R_2^4 R_1^2 - 3R_2^2 R_1^4 + 2R_2^6 R_1^4 - 3R_2^6 R_1^2 - R_2^4 - 3R_2^2 R_1^4 \ln R_2^2 \\ & + R_1^6 \ln R_1^2 - R_2^6 \ln R_2^2 - R_2^4 R_1^2 \ln \frac{R_2^2}{R_1^2} + 3R_2^4 R_1^2 \ln R_1^2 + 2R_2^2 R_1^2 \ln \frac{R_2^2}{R_1^2} \\ & + 2R_2^6 R_1^2 \ln \frac{R_2^2}{R_1^2} + 2R_2^4 R_1^4 \ln \frac{R_2^2}{R_1^2} + 2R_2^2 R_1^6 \ln \frac{R_2^2}{R_1^2} - R_2^4 R_1^6 \ln \frac{R_2^2}{R_1^2} \\ & \left. - 4R_2^2 R_1^4 \ln \frac{R_2^2}{R_1^2} - R_2^6 R_1^4 \ln \frac{R_2^2}{R_1^2} \right] \end{aligned}$$

$$\begin{aligned} f_{10}(R_1, R_2) = & \frac{3R_2^2}{2(1-R_2^2)^2(1-R_1^2)^2(R_1^2-R_2^2)} \left[-R_1^2 + R_1^4 + R_2^2 - R_2^2 R_1^4 \right. \\ & - R_2^4 + R_1^2 R_2^4 + 2R_1^2 \ln \frac{R_2^2}{R_1^2} - \ln \frac{R_2^2}{R_1^2} - R_1^4 \ln R_2^2 + 2R_2^2 \ln \frac{R_2^2}{R_1^2} \\ & \left. + 2R_2^2 R_1^4 \ln R_2^2 - 4R_2^2 R_1^2 \ln \frac{R_2^2}{R_1^2} + R_2^4 \ln R_1^2 - 2R_2^4 R_1^2 \ln R_1^2 \right] \end{aligned}$$

$$\begin{aligned} f_{11}(R_1, R_2) = & -\frac{4R_2^2}{(1-R_2^2)^2(1-R_1^2)^3(R_2^2-R_1^2)^2} \left[-R_1^2 + 4R_1^4 - 3R_1^6 + R_2^2 \right. \\ & - 3R_1^2 R_2^2 - 3R_1^4 R_2^2 + 5R_1^6 R_2^2 - R_2^4 + 6R_1^2 R_2^4 - 3R_1^4 R_2^4 - 2R_1^6 R_2^4 \\ & - 2R_2^6 R_1^2 + 2R_2^6 R_1^4 + 2R_1^6 \ln R_1^2 - R_2^2 \ln \frac{R_2^2}{R_1^2} + 3R_2^2 R_1^2 \ln \frac{R_2^2}{R_1^2} \\ & - 3R_2^2 R_1^4 \ln R_2^2 + R_2^2 R_1^6 \ln R_2^2 - 4R_2^2 R_1^6 \ln R_1^2 + 2R_2^4 \ln \frac{R_2^2}{R_1^2} - 6R_2^4 R_1^2 \ln \frac{R_2^2}{R_1^2} \\ & \left. + 6R_2^4 R_1^4 \ln R_2^2 - 2R_2^4 R_1^6 \ln \frac{R_2^2}{R_1^2} + R_2^6 \ln R_1^2 - 3R_2^6 R_1^2 \ln R_1^2 \right] \end{aligned}$$

$$\begin{aligned} f_{12}(R_1, R_2) = & \frac{4R_2^4}{R_1^2(1-R_2^2)^3(1-R_1^2)^2(R_1^2-R_2^2)^2} \left[3R_1^2 R_2^4 + 2R_1^6 R_2^2 + 3R_1^2 R_2^2 \right. \\ & - 6R_1^4 R_2^2 + 3R_1^4 R_2^4 - 2R_1^6 R_2^4 - 5R_1^2 R_2^6 + 2R_1^4 R_2^6 - R_1^2 + R_2^2 + R_1^4 \\ & - 4R_2^4 + 3R_2^6 + 3R_2^4 R_1^2 \ln R_1^2 - 4R_2^4 R_1^2 \ln R_2^2 - 6R_2^2 R_1^4 \ln R_2^2 \\ & + 6R_2^2 R_1^4 \ln R_1^2 + 3R_2^2 R_1^6 \ln R_2^2 + 4R_2^4 R_1^2 \ln R_2^2 - 6R_2^4 R_1^4 \ln R_1^2 \\ & + 4R_2^6 R_1^2 \ln R_2^2 - R_2^6 R_1^2 \ln R_1^2 - 2R_2^6 \ln R_2^2 - 2R_2^6 R_1^4 \ln \frac{R_2^2}{R_1^2} \\ & \left. + 3R_2^2 R_1^2 \ln \frac{R_2^2}{R_1^2} + 2R_1^4 \ln \frac{R_2^2}{R_1^2} - R_1^2 \ln \frac{R_2^2}{R_1^2} - R_1^6 \ln R_2^2 \right] \end{aligned}$$

$$\begin{aligned} f_{13}(R_1, R_2) = & -\frac{3R_2^2}{(1-R_2^2)^2(1-R_1^2)(R_1^2-R_2^2)^2} \left[R_1^4 - R_1^2 + R_2^2 - R_1^4 R_2^2 - R_2^4 \right. \\ & + R_1^2 R_2^4 + R_2^2 R_1^4 \ln R_2^2 - 2R_2^4 R_1^2 \ln R_2^2 + R_2^6 \ln R_1^2 - R_2^2 \ln \frac{R_2^2}{R_1^2} \\ & \left. + R_2^6 R_1^4 \ln R_2^2 - 2R_2^6 R_1^2 \ln R_1^2 \right] \end{aligned}$$

$$\begin{aligned}
& + 2R_2^4 \ln \frac{R_2^2}{R_1^2} \Big] \\
f_{14}(R_1, R_2) &= \frac{12R_2^4}{(1-R_2^2)^2(1-R_1^2)^2(R_1^2-R_2^2)^3} \left[3R_1^4 - 2R_1^2 - R_1^6 + 2R_2^2 + R_1^6 R_2^2 \right. \\
& - 3R_1^4 R_2^2 + 3R_2^4 + 3R_1^2 R_2^4 + R_2^6 - R_1^2 R_2^6 - R_1^6 \ln R_2^2 + 4R_2^2 R_1^4 \ln R_1^2 \\
& - R_2^2 R_1^4 \ln R_2^2 + R_2^4 R_1^2 \ln R_1^2 - 4R_2^4 R_1^2 \ln R_2^2 + R_2^6 \ln R_1^2 + 2R_1^4 \ln \frac{R_2^2}{R_1^2} \\
& - R_1^2 \ln \frac{R_2^2}{R_1^2} - R_2^2 \ln \frac{R_2^2}{R_1^2} + 2R_2^2 R_1^2 \ln \frac{R_2^2}{R_1^2} + 2R_2^4 R_1^4 \ln \frac{R_2^2}{R_1^2} + 2R_2^4 \ln \frac{R_2^2}{R_1^2} \Big] \\
f_{15}(R_1, R_2) &= \frac{6R_2^4}{R_1^2(1-R_2^2)^3(1-R_1^2)(R_1^2-R_2^2)^3} \left[-R_1^6 + R_1^4 - R_2^4 - 3R_1^2 R_2^4 \right. \\
& + R_1^6 R_2^4 + 3R_1^4 R_2^4 + 4R_2^6 - 4R_1^4 R_2^6 - 3R_2^8 + 3R_1^2 R_2^8 - 2R_2^2 R_1^6 \ln R_2^2 \\
& + 6R_2^4 R_1^4 \ln R_2^2 - 6R_2^6 R_1^2 \ln R_1^2 + 2R_2^8 \ln R_2^2 + 2R_2^2 R_1^2 \ln \frac{R_2^2}{R_1^2} \\
& - 6R_2^4 R_1^2 \ln \frac{R_2^2}{R_1^2} - 2R_2^8 R_1^2 \ln \frac{R_2^2}{R_1^2} \Big] \\
f_1(R) &= f_1(R, R) = \frac{2}{(1-R^2)^2} [1 - R^2 + R^2 \ln R^2] \\
f_2(R) &= \frac{3}{(1-R^2)^3} [1 - R^4 + 2R^2 \ln R^2] \\
f_3(R) &= \frac{2}{(1-R^2)^4} [2 + R^6 - 6R^4 + 3R^2 + 6R^2 \ln R^2] \\
f_4(R) &= \frac{2}{(1-R^2)^4} [1 - 6R^2 + 3R^4 + 2R^6 - 6R^4 \ln R^2] \\
g_1(R) &= \frac{1}{(1-R^2)} [1 - R^2 + R^2 \ln R^2] \\
g_2(R) &= \frac{1}{4(1-R^2)^2} [-3 + 4R^2 - R^4 - 4R^2 \ln R^2 + 2R^4 \ln R^2] . \\
\end{aligned} \tag{B.9}$$

Note that in the special case $M_{\tilde{g}} = M_S = \tilde{M}_S$, $R_t = R_b = 1$, the functions above are normalized as $f_i(1, 1) = 1$, $f_i(1) = 1$ and $g_i(1) = 0$. Notice also that we use here the same notation as in ref [10].

B.2 Near-zero sbottom and stop mixing

The loop integrals are expanded as follows:

$$\begin{aligned}
C_0(m_t^2, M_{H^+}^2, m_b^2; M_{\tilde{g}}^2, M_{\tilde{t}_i}^2, M_{\tilde{b}_j}^2) &\simeq -\frac{1}{2M_{\tilde{t}_i}^2} f_1(R_{t_i}, R_{b_j}) \\
& - \frac{m_t^2}{24M_{\tilde{t}_i}^4} f_2(R_{t_i}, R_{b_j}) - \frac{M_{H^+}^2}{24M_{\tilde{t}_i}^4} f_3(R_{t_i}, R_{b_j}) - \frac{m_b^2}{24M_{\tilde{t}_i}^4} f_4(R_{t_i}, R_{b_j}) ,
\end{aligned}$$

$$\begin{aligned}
C_{11}(m_t^2, M_{H^+}^2, m_b^2; M_{\tilde{g}}^2, M_{\tilde{t}_i}^2, M_{\tilde{b}_j}^2) &\simeq \frac{1}{3M_{\tilde{t}_i}^2} f_{10}(R_{t_i}, R_{b_j}), \\
C_{12}(m_t^2, M_{H^+}^2, m_b^2; M_{\tilde{g}}^2, M_{\tilde{t}_i}^2, M_{\tilde{b}_j}^2) &\simeq \frac{1}{6M_{\tilde{t}_i}^2} f_{13}(R_{t_i}, R_{b_j}), \\
B_0(m_q^2; M_{\tilde{q}_i}^2, M_{\tilde{g}}^2) &\simeq \Delta - \ln \frac{M_{\tilde{q}_i}^2}{\mu_0^2} + g_1(R_{q_i}) + \frac{m_q^2}{6M_{\tilde{q}_i}^2} f_2(R_{q_i}), \\
B_1(m_q^2; M_{\tilde{q}_i}^2, M_{\tilde{g}}^2) &\simeq -\frac{1}{2}(\Delta - \ln \frac{M_{\tilde{q}_i}^2}{\mu_0^2}) + g_2(R_{q_i}) - \frac{m_q^2}{12M_{\tilde{q}_i}^2} f_3(R_{q_i}).
\end{aligned} \tag{B.10}$$

Where $R_{q_i} \equiv M_{\tilde{g}}/M_{\tilde{q}_i}$ ($i = 1, 2$) and the functions f_i and g_i are the same as in Section B.1.

B.3 Maximal sbottom mixing and near-zero stop mixing

The loop integrals are expanded as follows:

$$\begin{aligned}
C_0(m_t^2, M_{H^+}^2, m_b^2; M_{\tilde{g}}^2, M_{\tilde{t}_i}^2, M_{\tilde{b}_j}^2) &\simeq -\frac{1}{2M_{\tilde{t}_i}^2} f_1(R_{t_i}, R_b) \\
&\quad - \frac{m_t^2}{24M_{\tilde{t}_i}^4} f_2(R_{t_i}, R_b) - \frac{M_{H^+}^2}{24M_{\tilde{t}_i}^4} f_3(R_{t_i}, R_b) - \frac{m_b^2}{24M_{\tilde{t}_i}^4} f_4(R_{t_i}, R_b) \\
&\quad - (-1)^j \frac{\Delta_b^2}{6M_{\tilde{t}_i}^4} f_6(R_{t_i}, R_b) - \frac{\Delta_b^4}{12M_{\tilde{t}_i}^6} f_8(R_{t_i}, R_b), \\
C_{11}(m_t^2, M_{H^+}^2, m_b^2; M_{\tilde{g}}^2, M_{\tilde{t}_i}^2, M_{\tilde{b}_j}^2) &\simeq \frac{1}{3M_{\tilde{t}_i}^2} f_{10}(R_{t_i}, R_b) + (-1)^j \frac{\Delta_b^2}{8M_{\tilde{t}_i}^4} f_{12}(R_{t_i}, R_b), \\
C_{12}(m_t^2, M_{H^+}^2, m_b^2; M_{\tilde{g}}^2, M_{\tilde{t}_i}^2, M_{\tilde{b}_j}^2) &\simeq \frac{1}{6M_{\tilde{t}_i}^2} f_{13}(R_{t_i}, R_b) + (-1)^j \frac{\Delta_b^2}{12M_{\tilde{t}_i}^4} f_{15}(R_{t_i}, R_b).
\end{aligned} \tag{B.11}$$

Here $R_{t_i} \equiv M_{\tilde{g}}/M_{\tilde{t}_i}$ ($i = 1, 2$); $R_b \equiv M_{\tilde{g}}/\tilde{M}_S$ and the functions f_i are the same as in Section B.1. For the two-point integrals $B_{0,1}(m_b^2, M_{\tilde{g}}^2, M_{\tilde{b}_i}^2)$ and $B_{0,1}(m_t^2, M_{\tilde{g}}^2, M_{\tilde{t}_i}^2)$ we use the expressions given in (B.8) and (B.10) respectively.

B.4 Maximal stop mixing and near-zero sbottom mixing

The loop integrals are expanded as follows:

$$\begin{aligned}
C_0(m_t^2, M_{H^+}^2, m_b^2; M_{\tilde{g}}^2, M_{\tilde{t}_i}^2, M_{\tilde{b}_j}^2) &\simeq -\frac{1}{2M_S^2} f_1(R_t, R_{b_j}) - \frac{m_t^2}{24M_S^4} f_2(R_t, R_{b_j}) - \frac{M_{H^+}^2}{24M_S^4} f_3(R_t, R_{b_j}) - \frac{m_b^2}{24M_S^4} f_4(R_t, R_{b_j}) \\
&\quad - (-1)^i \frac{\Delta_t^2}{6M_S^4} f_5(R_t, R_{b_j}) - \frac{\Delta_t^4}{12M_S^6} f_7(R_t, R_{b_j}),
\end{aligned}$$

$$\begin{aligned}
C_{11}(m_t^2, M_{H^+}^2, m_b^2; M_{\tilde{g}}^2, M_{\tilde{t}_i}^2, M_{\tilde{b}_j}^2) &\simeq \frac{1}{3M_S^2} f_{10}(R_t, R_{b_j}) + (-1)^i \frac{\Delta_t^2}{8M_S^4} f_{11}(R_t, R_{b_j}), \\
C_{12}(m_t^2, M_{H^+}^2, m_b^2; M_{\tilde{g}}^2, M_{\tilde{t}_i}^2, M_{\tilde{b}_j}^2) &\simeq \frac{1}{6M_S^2} f_{13}(R_t, R_{b_j}) + (-1)^i \frac{\Delta_t^2}{24M_S^4} f_{14}(R_t, R_{b_j}),
\end{aligned} \tag{B.12}$$

where $R_{b_i} \equiv M_{\tilde{g}}/M_{\tilde{b}_i}$ ($i = 1, 2$); $R_t \equiv M_{\tilde{g}}/M_S$ and again the functions f_i are as in Section B.1. In this case for the two-point integrals $B_{0,1}(m_b^2, M_{\tilde{g}}^2, M_{\tilde{b}_i}^2)$ and $B_{0,1}(m_t^2, M_{\tilde{g}}^2, M_{\tilde{t}_i}^2)$ we use the expressions given in (B.10) and (B.8) respectively.

C Complete expressions for Δ_{SQCD} to order M_{EW}^2/M_{SUSY}^2

Here we give the complete expressions for the expansion of the SUSY-QCD correction to $\Gamma(H^+ \rightarrow t\bar{b})$ up to order M_{EW}^2/M_{SUSY}^2 . From eqs. (12), (15) and (16) the SUSY-QCD correction can be rewritten as:

$$\Delta_{SQCD} = \frac{U_t}{D}(K_t + H_t) + \frac{U_b}{D}(K_b + H_b), \tag{C.13}$$

where we have defined:

$$\begin{aligned}
K_t &= \frac{\delta m_t}{m_t} + \frac{1}{2} \delta Z_L^b + \frac{1}{2} \delta Z_R^t, \\
K_b &= \frac{\delta m_b}{m_b} + \frac{1}{2} \delta Z_L^t + \frac{1}{2} \delta Z_R^b.
\end{aligned} \tag{C.14}$$

In the following we give the expressions for K_t , H_t , K_b and H_b up to order M_{EW}^2/M_{SUSY}^2 in the four different cases that we have considered in this paper.

C.1 Maximal stop and sbottom mixing

The results for K_t , H_t , K_b and H_b up to order M_{EW}^2/M_{SUSY}^2 are the following:

$$\begin{aligned}
K_t &= \frac{\alpha_s}{3\pi} \left[M_{\tilde{g}} \left(\frac{X_t}{M_S^2} f_1(R_t) - \frac{m_b^2 X_b}{6 \tilde{M}_S^4} (2f_3 - f_4)(R_b) \right) - \frac{1}{2} \ln \frac{R_b^2}{R_t^2} + g_1(R_t) - g_1(R_b) \right. \\
&\quad + g_2(R_t) - g_2(R_b) - \frac{m_t^2}{12M_S^2} (2f_2 - f_3)(R_t) - \frac{m_b^2}{4\tilde{M}_S^2} (2f_2 - f_3)(R_b) \\
&\quad + \frac{m_t^2 X_t^2}{24M_S^4} (4f_2 - 2f_3 + f_4)(R_t) - \frac{m_b^2 X_b^2}{24\tilde{M}_S^4} (4f_2 - 2f_3 + f_4)(R_b) \\
&\quad \left. - \frac{M_L^2 - M_R^2}{12M_S^2} (3f_1 - f_2)(R_t) + \frac{M_L'^2 - M_R'^2}{12\tilde{M}_S^2} (3f_1 - f_2)(R_b) \right],
\end{aligned}$$

$$\begin{aligned}
H_t &= -\frac{2\alpha_s}{3\pi} \frac{1}{m_t \cot \beta} \left[-\frac{M_{\tilde{g}} g_{RL}}{2M_S^2} f_1(R_t, R_b) + \frac{m_t g_{LL}}{6M_S^2} (2f_{10} - f_{13})(R_t, R_b) \right. \\
&\quad + \frac{M_{\tilde{g}} g_{LL}}{6M_S^4} m_t X_t f_5(R_t, R_b) + \frac{m_b g_{RR}}{6M_S^2} f_{13}(R_t, R_b) + \frac{M_{\tilde{g}} g_{RR}}{6M_S^4} m_b X_b f_6(R_t, R_b) \\
&\quad - \frac{m_t m_b X_b g_{LR}}{24M_S^4} (3f_{12} - 2f_{15})(R_t, R_b) - \frac{m_t m_b X_t g_{LR}}{24M_S^4} f_{14}(R_t, R_b) \\
&\quad - \frac{M_{\tilde{g}} m_t m_b X_t X_b g_{LR}}{12M_S^6} f_9(R_t, R_b) + \frac{m_t^2 X_t g_{RL}}{24M_S^4} (f_{14} - 3f_{11})(R_t, R_b) \\
&\quad - \frac{m_b^2 X_b g_{RL}}{12M_S^4} f_{15}(R_t, R_b) - \frac{M_{\tilde{g}} g_{RL}}{24M_S^4} (m_t^2 f_2 + M_{H^+}^2 f_3 + m_b^2 f_4)(R_t, R_b) \\
&\quad - \frac{M_{\tilde{g}} m_t^2 X_t^2 g_{RL}}{12M_S^6} f_7(R_t, R_b) - \frac{M_{\tilde{g}} m_b^2 X_b^2 g_{RL}}{12M_S^6} f_8(R_t, R_b) \\
&\quad \left. + \frac{M_{\tilde{g}} (M_L'^2 - M_R'^2) g_{RL}}{12M_S^4} f_6(R_t, R_b) - \frac{M_{\tilde{g}} (M_L^2 - M_R^2) g_{RL}}{12M_S^4} f_5(R_t, R_b) \right], \\
K_b &= \frac{\alpha_s}{3\pi} \left[M_{\tilde{g}} \left(\frac{X_b}{\tilde{M}_S^2} f_1(R_b) - \frac{m_t^2 X_t}{6M_S^4} (2f_3 - f_4)(R_t) \right) + \frac{1}{2} \ln \frac{R_b^2}{R_t^2} - g_1(R_t) + g_1(R_b) \right. \\
&\quad - g_2(R_t) + g_2(R_b) - \frac{m_b^2}{12\tilde{M}_S^2} (2f_2 - f_3)(R_b) - \frac{m_t^2}{4M_S^2} (2f_2 - f_3)(R_t) \\
&\quad - \frac{m_t^2 X_t^2}{24M_S^4} (4f_2 - 2f_3 + f_4)(R_t) + \frac{m_b^2 X_b^2}{24\tilde{M}_S^4} (4f_2 - 2f_3 + f_4)(R_b) \\
&\quad \left. + \frac{M_L^2 - M_R^2}{12M_S^2} (3f_1 - f_2)(R_t) - \frac{M_L'^2 - M_R'^2}{12\tilde{M}_S^2} (3f_1 - f_2)(R_b) \right], \\
H_b &= -\frac{2\alpha_s}{3\pi} \frac{1}{m_b \tan \beta} \left[-\frac{M_{\tilde{g}} g_{LR}}{2M_S^2} f_1(R_t, R_b) + \frac{m_t g_{RR}}{6M_S^2} (2f_{10} - f_{13})(R_t, R_b) \right. \\
&\quad + \frac{M_{\tilde{g}} g_{RR}}{6M_S^4} m_t X_t f_5(R_t, R_b) + \frac{m_b g_{LL}}{6M_S^2} f_{13}(R_t, R_b) + \frac{M_{\tilde{g}} g_{LL}}{6M_S^4} m_b X_b f_6(R_t, R_b) \\
&\quad - \frac{m_t m_b X_b g_{RL}}{24M_S^4} (3f_{12} - 2f_{15})(R_t, R_b) - \frac{m_t m_b X_t g_{RL}}{24M_S^4} f_{14}(R_t, R_b) \\
&\quad - \frac{M_{\tilde{g}} m_t m_b X_t X_b g_{RL}}{12M_S^6} f_9(R_t, R_b) + \frac{m_t^2 X_t g_{LR}}{24M_S^4} (f_{14} - 3f_{11})(R_t, R_b) \\
&\quad - \frac{m_b^2 X_b g_{LR}}{12M_S^4} f_{15}(R_t, R_b) - \frac{M_{\tilde{g}} g_{LR}}{24M_S^4} (m_t^2 f_2 + M_{H^+}^2 f_3 + m_b^2 f_4)(R_t, R_b) \\
&\quad - \frac{M_{\tilde{g}} m_t^2 X_t^2 g_{LR}}{12M_S^6} f_7(R_t, R_b) - \frac{M_{\tilde{g}} m_b^2 X_b^2 g_{LR}}{12M_S^6} f_8(R_t, R_b) \\
&\quad \left. - \frac{M_{\tilde{g}} (M_L'^2 - M_R'^2) g_{LR}}{12M_S^4} f_6(R_t, R_b) + \frac{M_{\tilde{g}} (M_L^2 - M_R^2) g_{LR}}{12M_S^4} f_5(R_t, R_b) \right], \quad (C.15)
\end{aligned}$$

C.2 Near-zero stop and sbottom mixing

The results for K_t , H_t , K_b and H_b up to order M_{EW}^2/M_{SUSY}^2 are:

$$\begin{aligned}
K_t &= \frac{\alpha_s}{3\pi} \left[-\frac{2M_{\tilde{g}}X_t}{M_{\tilde{t}_1}^2 - M_{\tilde{t}_2}^2} \left(\ln \frac{M_{\tilde{t}_2}^2}{M_{\tilde{t}_1}^2} + g_1(R_{t_1}) - g_1(R_{t_2}) \right) - \frac{1}{2} \ln \frac{M_{\tilde{t}_1}^2}{M_{\tilde{b}_1}^2} + g_1(R_{t_1}) \right. \\
&\quad - g_1(R_{b_1}) + g_2(R_{t_1}) - g_2(R_{b_1}) + \frac{m_t^2 X_t^2}{(M_{\tilde{t}_1}^2 - M_{\tilde{t}_2}^2)^2} \left(-\frac{1}{2} \ln \frac{M_{\tilde{t}_2}^2}{M_{\tilde{t}_1}^2} + g_1(R_{t_2}) - g_1(R_{t_1}) \right. \\
&\quad \left. \left. + g_2(R_{t_2}) - g_2(R_{t_1}) \right) - \frac{m_b^2 X_b^2}{(M_{\tilde{b}_1}^2 - M_{\tilde{b}_2}^2)^2} \left(-\frac{1}{2} \ln \frac{M_{\tilde{b}_2}^2}{M_{\tilde{b}_1}^2} + g_1(R_{b_2}) - g_1(R_{b_1}) + g_2(R_{b_2}) \right. \\
&\quad \left. - g_2(R_{b_1}) \right) - \frac{m_b^2}{6M_{\tilde{b}_1}^2} (2f_2 - f_3)(R_{b_1}) - \frac{m_t^2}{12M_{\tilde{t}_2}^2} (2f_2 - f_3)(R_{t_2}) \right. \\
&\quad \left. - \frac{m_b^2}{12M_{\tilde{b}_2}^2} (2f_2 - f_3)(R_{b_2}) + \frac{M_{\tilde{g}} m_b^2 X_b}{M_{\tilde{b}_1}^2 - M_{\tilde{b}_2}^2} \left(\frac{f_2(R_{b_1})}{3M_{\tilde{b}_1}^2} - \frac{f_2(R_{b_2})}{3M_{\tilde{b}_2}^2} \right) \right], \\
H_t &= -\frac{2\alpha_s}{3\pi} \frac{1}{m_t \cot \beta} \left[-\frac{M_{\tilde{g}} g_{RL}}{2M_{\tilde{t}_2}^2} f_1(R_{t_2}, R_{b_1}) + \frac{m_t g_{LL}}{6M_{\tilde{t}_1}^2} (2f_{10} - f_{13})(R_{t_1}, R_{b_1}) \right. \\
&\quad + \frac{M_{\tilde{g}} m_t X_t}{M_{\tilde{t}_1}^2 - M_{\tilde{t}_2}^2} \left(g_{LL} + \frac{m_t X_t}{M_{\tilde{t}_1}^2 - M_{\tilde{t}_2}^2} g_{RL} \right) \left(\frac{f_1(R_{t_2}, R_{b_1})}{2M_{\tilde{t}_2}^2} - \frac{f_1(R_{t_1}, R_{b_1})}{2M_{\tilde{t}_1}^2} \right) \\
&\quad + \frac{M_{\tilde{g}} m_b X_b}{M_{\tilde{b}_1}^2 - M_{\tilde{b}_2}^2} \left(g_{RR} - \frac{m_b X_b}{M_{\tilde{b}_1}^2 - M_{\tilde{b}_2}^2} g_{RL} \right) \left(\frac{f_1(R_{t_2}, R_{b_2})}{2M_{\tilde{t}_2}^2} - \frac{f_1(R_{t_1}, R_{b_1})}{2M_{\tilde{t}_1}^2} \right) \\
&\quad - \frac{m_t m_b X_b g_{LR}}{6M_{\tilde{t}_1}^2 (M_{\tilde{b}_1}^2 - M_{\tilde{b}_2}^2)} (f_{13}(R_{t_1}, R_{b_1}) - f_{13}(R_{t_1}, R_{b_2}) - 2(f_{10}(R_{t_1}, R_{b_1}) - f_{10}(R_{t_1}, R_{b_2}))) \\
&\quad - \frac{m_t m_b X_t g_{LR}}{M_{\tilde{t}_1}^2 - M_{\tilde{t}_2}^2} \left(\frac{f_{13}(R_{t_2}, R_{b_2})}{6M_{\tilde{t}_2}^2} - \frac{f_{13}(R_{t_1}, R_{b_2})}{6M_{\tilde{t}_1}^2} \right) + \frac{m_b g_{RR}}{6M_{\tilde{t}_2}^2} f_{13}(R_{t_2}, R_{b_2}) \\
&\quad + \frac{M_{\tilde{g}} m_t m_b X_t X_b g_{LR}}{(M_{\tilde{t}_1}^2 - M_{\tilde{t}_2}^2)(M_{\tilde{b}_1}^2 - M_{\tilde{b}_2}^2)} \left(\frac{f_1(R_{t_1}, R_{b_2})}{2M_{\tilde{t}_1}^2} + \frac{f_1(R_{t_2}, R_{b_1})}{2M_{\tilde{t}_2}^2} - \frac{f_1(R_{t_1}, R_{b_1})}{2M_{\tilde{t}_1}^2} - \frac{f_1(R_{t_2}, R_{b_2})}{2M_{\tilde{t}_2}^2} \right) \\
&\quad - \frac{m_t^2 X_t g_{RL}}{M_{\tilde{t}_1}^2 - M_{\tilde{t}_2}^2} \left(\frac{f_{13}(R_{t_1}, R_{b_1})}{6M_{\tilde{t}_1}^2} - \frac{f_{10}(R_{t_1}, R_{b_1})}{3M_{\tilde{t}_1}^2} - \frac{f_{13}(R_{t_2}, R_{b_1})}{6M_{\tilde{t}_2}^2} + \frac{f_{10}(R_{t_2}, R_{b_1})}{3M_{\tilde{t}_2}^2} \right) \\
&\quad - \frac{m_b^2 X_b g_{RL}}{6M_{\tilde{t}_2}^2 (M_{\tilde{b}_1}^2 - M_{\tilde{b}_2}^2)} (f_{13}(R_{t_2}, R_{b_2}) - f_{13}(R_{t_2}, R_{b_1})) \\
&\quad \left. - \frac{M_{\tilde{g}} g_{RL}}{24M_{\tilde{t}_2}^4} (m_t^2 f_2 + M_{H^+}^2 f_3 + m_b^2 f_4)(R_{t_2}, R_{b_1}) \right], \\
K_b &= \frac{\alpha_s}{3\pi} \left[-\frac{2M_{\tilde{g}} X_b}{M_{\tilde{b}_1}^2 - M_{\tilde{b}_2}^2} \left(\ln \frac{M_{\tilde{b}_2}^2}{M_{\tilde{b}_1}^2} + g_1(R_{b_1}) - g_1(R_{b_2}) \right) - \frac{1}{2} \ln \frac{M_{\tilde{b}_1}^2}{M_{\tilde{t}_1}^2} + g_1(R_{b_1}) \right.
\end{aligned}$$

$$\begin{aligned}
& - g_1(R_{t_1}) + g_2(R_{b_1}) - g_2(R_{t_1}) - \frac{m_t^2 X_t^2}{(M_{\tilde{t}_1}^2 - M_{\tilde{t}_2}^2)^2} \left(-\frac{1}{2} \ln \frac{M_{\tilde{t}_2}^2}{M_{\tilde{t}_1}^2} + g_1(R_{t_2}) - g_1(R_{t_1}) \right. \\
& + g_2(R_{t_2}) - g_2(R_{t_1}) \left. \right) + \frac{m_b^2 X_b^2}{(M_{\tilde{b}_1}^2 - M_{\tilde{b}_2}^2)^2} \left(-\frac{1}{2} \ln \frac{M_{\tilde{b}_2}^2}{M_{\tilde{b}_1}^2} + g_1(R_{b_2}) - g_1(R_{b_1}) + g_2(R_{b_2}) \right. \\
& - g_2(R_{b_1}) \left. \right) - \frac{m_t^2}{6M_{\tilde{t}_1}^2} (2f_2 - f_3)(R_{t_1}) - \frac{m_b^2}{12M_{\tilde{b}_2}^2} (2f_2 - f_3)(R_{b_2}) \\
& - \frac{m_t^2}{12M_{\tilde{t}_2}^2} (2f_2 - f_3)(R_{t_2}) + \frac{M_{\tilde{g}} m_t^2 X_t}{M_{\tilde{t}_1}^2 - M_{\tilde{t}_2}^2} \left(\frac{f_2(R_{t_1})}{3M_{\tilde{t}_1}^2} - \frac{f_2(R_{t_2})}{3M_{\tilde{t}_2}^2} \right) \Big] , \\
H_b = & -\frac{2\alpha_s}{3\pi} \frac{1}{m_b \tan \beta} \left[-\frac{M_{\tilde{g}} g_{LR}}{2M_{\tilde{t}_1}^2} f_1(R_{t_1}, R_{b_2}) + \frac{m_t g_{RR}}{6M_{\tilde{t}_2}^2} (2f_{10} - f_{13})(R_{t_2}, R_{b_2}) \right. \\
& + \frac{M_{\tilde{g}} m_t X_t}{M_{\tilde{t}_1}^2 - M_{\tilde{t}_2}^2} \left(g_{RR} - \frac{m_t X_t}{M_{\tilde{t}_1}^2 - M_{\tilde{t}_2}^2} g_{LR} \right) \left(\frac{f_1(R_{t_2}, R_{b_2})}{2M_{\tilde{t}_2}^2} - \frac{f_1(R_{t_1}, R_{b_2})}{2M_{\tilde{t}_1}^2} \right) \\
& + \frac{M_{\tilde{g}} m_b X_b}{M_{\tilde{b}_1}^2 - M_{\tilde{b}_2}^2} \left(g_{LL} + \frac{m_b X_b}{M_{\tilde{b}_1}^2 - M_{\tilde{b}_2}^2} g_{LR} \right) \left(\frac{f_1(R_{t_1}, R_{b_2})}{2M_{\tilde{t}_1}^2} - \frac{f_1(R_{t_1}, R_{b_1})}{2M_{\tilde{t}_1}^2} \right) \\
& - \frac{m_t m_b X_b g_{RL}}{6M_{\tilde{t}_2}^2 (M_{\tilde{b}_1}^2 - M_{\tilde{b}_2}^2)} (f_{13}(R_{t_2}, R_{b_1}) - 2f_{10}(R_{t_2}, R_{b_1}) - f_{13}(R_{t_2}, R_{b_2}) + 2f_{10}(R_{t_2}, R_{b_2})) \\
& - \frac{m_t m_b X_t g_{RL}}{M_{\tilde{t}_1}^2 - M_{\tilde{t}_2}^2} \left(\frac{f_{13}(R_{t_2}, R_{b_1})}{6M_{\tilde{t}_2}^2} - \frac{f_{13}(R_{t_1}, R_{b_1})}{6M_{\tilde{t}_1}^2} \right) + \frac{m_b g_{LL}}{6M_{\tilde{t}_1}^2} f_{13}(R_{t_1}, R_{b_1}) \\
& - \frac{M_{\tilde{g}} m_t m_b X_t X_b g_{RL}}{(M_{\tilde{t}_1}^2 - M_{\tilde{t}_2}^2)(M_{\tilde{b}_1}^2 - M_{\tilde{b}_2}^2)} \left(\frac{f_1(R_{t_1}, R_{b_1})}{2M_{\tilde{t}_1}^2} - \frac{f_1(R_{t_1}, R_{b_2})}{2M_{\tilde{t}_1}^2} - \frac{f_1(R_{t_2}, R_{b_2})}{2M_{\tilde{t}_2}^2} + \frac{f_1(R_{t_2}, R_{b_1})}{2M_{\tilde{t}_2}^2} \right) \\
& - \frac{m_t^2 X_t g_{LR}}{M_{\tilde{t}_1}^2 - M_{\tilde{t}_2}^2} \left(\frac{f_{13}(R_{t_1}, R_{b_2})}{6M_{\tilde{t}_1}^2} - \frac{f_{10}(R_{t_1}, R_{b_2})}{3M_{\tilde{t}_1}^2} - \frac{f_{13}(R_{t_2}, R_{b_2})}{6M_{\tilde{t}_2}^2} + \frac{f_{10}(R_{t_2}, R_{b_2})}{3M_{\tilde{t}_2}^2} \right) \\
& - \frac{m_b^2 X_b g_{LR}}{6M_{\tilde{t}_1}^2 (M_{\tilde{b}_1}^2 - M_{\tilde{b}_2}^2)} (f_{13}(R_{t_1}, R_{b_2}) - f_{13}(R_{t_1}, R_{b_1})) \\
& - \frac{M_{\tilde{g}} g_{LR}}{24M_{\tilde{t}_1}^4} (m_t^2 f_2 + M_{H^+}^2 f_3 + m_b^2 f_4)(R_{t_1}, R_{b_2}) \Big] , \tag{C.16}
\end{aligned}$$

C.3 Maximal sbottom mixing and near-zero stop mixing

The results for K_t , H_t , K_b and H_b up to order M_{EW}^2/M_{SUSY}^2 are:

$$\begin{aligned}
K_t = & \frac{\alpha_s}{3\pi} \left[-\frac{2M_{\tilde{g}} X_t}{M_{\tilde{t}_1}^2 - M_{\tilde{t}_2}^2} \left(\ln \frac{M_{\tilde{t}_2}^2}{M_{\tilde{t}_1}^2} + g_1(R_{t_1}) - g_1(R_{t_2}) \right) - \frac{1}{2} \ln \frac{M_{\tilde{t}_1}^2}{\tilde{M}_S^2} + g_1(R_{t_1}) \right. \\
& - g_1(R_b) + g_2(R_{t_1}) - g_2(R_b) + \frac{m_t^2 X_t^2}{(M_{\tilde{t}_1}^2 - M_{\tilde{t}_2}^2)^2} \left(-\frac{1}{2} \ln \frac{M_{\tilde{t}_2}^2}{M_{\tilde{t}_1}^2} + g_1(R_{t_2}) - g_1(R_{t_1}) \right. \\
& \left. \left. \right) \right]
\end{aligned}$$

$$\begin{aligned}
& + g_2(R_{t_2}) - g_2(R_{t_1})) - \frac{m_t^2}{12M_{t_2}^2}(2f_2 - f_3)(R_{t_2}) - \frac{m_b^2}{4\tilde{M}_S^2}(2f_2 - f_3)(R_b) \\
& - \frac{m_b^2 X_b^2}{24\tilde{M}_S^4}(4f_2 - 2f_3 + f_4)(R_b) + \frac{M_L'^2 - M_R'^2}{12\tilde{M}_S^2}(3f_1 - f_2)(R_b) - \frac{M_{\tilde{g}} m_b^2 X_b}{6\tilde{M}_S^4}(2f_3 - f_4)(R_b) \Big] ,
\end{aligned}$$

$$\begin{aligned}
H_t = & -\frac{2\alpha_s}{3\pi} \frac{1}{m_t \cot \beta} \left[-\frac{M_{\tilde{g}} g_{RL}}{2M_{\tilde{t}_2}^2} f_1(R_{t_2}, R_b) + \frac{m_t g_{LL}}{6M_{\tilde{t}_1}^2}(2f_{10} - f_{13})(R_{t_1}, R_b) \right. \\
& + \frac{M_{\tilde{g}} m_t X_t}{M_{\tilde{t}_1}^2 - M_{\tilde{t}_2}^2} \left(g_{LL} + \frac{m_t X_t}{M_{\tilde{t}_1}^2 - M_{\tilde{t}_2}^2} g_{RL} \right) \left(\frac{f_1(R_{t_2}, R_b)}{2M_{\tilde{t}_2}^2} - \frac{f_1(R_{t_1}, R_b)}{2M_{\tilde{t}_1}^2} \right) \\
& + \frac{m_b g_{RR}}{6M_{\tilde{t}_2}^2} f_{13}(R_{t_2}, R_b) + \frac{M_{\tilde{g}} g_{RR}}{6M_{\tilde{t}_2}^4} m_b X_b f_6(R_{t_2}, R_b) \\
& - \frac{m_t m_b X_b g_{LR}}{24M_{\tilde{t}_1}^4} (3f_{12}(R_{t_1}, R_b) - 2f_{15}(R_{t_1}, R_b)) \\
& - \frac{m_t m_b X_t g_{LR}}{M_{\tilde{t}_1}^2 - M_{\tilde{t}_2}^2} \left(\frac{f_{13}(R_{t_2}, R_b)}{6M_{\tilde{t}_2}^2} - \frac{f_{13}(R_{t_1}, R_b)}{6M_{\tilde{t}_1}^2} \right) \\
& + \frac{M_{\tilde{g}} m_t m_b X_t X_b g_{LR}}{(M_{\tilde{t}_1}^2 - M_{\tilde{t}_2}^2)} \left(\frac{f_6(R_{t_1}, R_b)}{6M_{\tilde{t}_1}^4} - \frac{f_6(R_{t_2}, R_b)}{6M_{\tilde{t}_2}^4} \right) \\
& - \frac{m_t^2 X_t g_{RL}}{M_{\tilde{t}_1}^2 - M_{\tilde{t}_2}^2} \left(\frac{f_{13}(R_{t_1}, R_b)}{6M_{\tilde{t}_1}^2} - \frac{f_{10}(R_{t_1}, R_b)}{3M_{\tilde{t}_1}^2} - \frac{f_{13}(R_{t_2}, R_b)}{6M_{\tilde{t}_2}^2} + \frac{f_{10}(R_{t_2}, R_b)}{3M_{\tilde{t}_2}^2} \right) \\
& - \frac{m_b^2 X_b g_{RL}}{12M_{\tilde{t}_2}^4} f_{15}(R_{t_2}, R_b) - \frac{M_{\tilde{g}} g_{RL}}{24M_{\tilde{t}_2}^4} (m_t^2 f_2 + M_{H^+}^2 f_3 + m_b^2 f_4)(R_{t_2}, R_b) \\
& \left. - \frac{M_{\tilde{g}} m_b^2 X_b^2 g_{RL}}{12M_{\tilde{t}_2}^6} f_8(R_{t_2}, R_b) + \frac{M_{\tilde{g}} (M_L'^2 - M_R'^2) g_{RL}}{12M_{\tilde{t}_2}^4} f_6(R_{t_2}, R_b) \right] ,
\end{aligned}$$

$$\begin{aligned}
K_b = & \frac{\alpha_s}{3\pi} \left[\frac{M_{\tilde{g}} X_b}{\tilde{M}_S^2} f_1(R_b) + \frac{1}{2} \ln \frac{M_{\tilde{t}_1}^2}{\tilde{M}_S^2} - g_1(R_{t_1}) + g_1(R_b) - g_2(R_{t_1}) + g_2(R_b) \right. \\
& - \frac{m_t^2 X_t^2}{(M_{\tilde{t}_1}^2 - M_{\tilde{t}_2}^2)^2} \left(-\frac{1}{2} \ln \frac{M_{\tilde{t}_2}^2}{M_{\tilde{t}_1}^2} + g_1(R_{t_2}) - g_1(R_{t_1}) + g_2(R_{t_2}) - g_2(R_{t_1}) \right) \\
& - \frac{m_t^2}{12M_{\tilde{t}_2}^2} (2f_2 - f_3)(R_{t_2}) - \frac{m_b^2}{12\tilde{M}_S^2} (2f_2 - f_3)(R_b) \\
& + \frac{m_b^2 X_b^2}{24\tilde{M}_S^4} (4f_2 - 2f_3 + f_4)(R_b) - \frac{M_L'^2 - M_R'^2}{12\tilde{M}_S^2} (3f_1 - f_2)(R_b) \\
& \left. + \frac{M_{\tilde{g}} m_t^2 X_t}{M_{\tilde{t}_1}^2 - M_{\tilde{t}_2}^2} \left(\frac{f_2(R_{t_1})}{3M_{\tilde{t}_1}^2} - \frac{f_2(R_{t_2})}{3M_{\tilde{t}_2}^2} \right) - \frac{m_t^2}{6M_{\tilde{t}_1}^2} (2f_2 - f_3)(R_{t_1}) \right] ,
\end{aligned}$$

$$H_b = -\frac{2\alpha_s}{3\pi} \frac{1}{m_b \tan \beta} \left[-\frac{M_{\tilde{g}} g_{LR}}{2M_{\tilde{t}_1}^2} f_1(R_{t_1}, R_b) + \frac{m_t g_{RR}}{6M_{\tilde{t}_2}^2} (2f_{10} - f_{13})(R_{t_2}, R_b) \right.$$

$$\begin{aligned}
& + \frac{M_{\tilde{g}} m_t X_t}{M_{\tilde{t}_1}^2 - M_{\tilde{t}_2}^2} \left(g_{RR} - \frac{m_t X_t}{M_{\tilde{t}_1}^2 - M_{\tilde{t}_2}^2} g_{LR} \right) \left(\frac{f_1(R_{t_2}, R_b)}{2M_{\tilde{t}_2}^2} - \frac{f_1(R_{t_1}, R_b)}{2M_{\tilde{t}_1}^2} \right) \\
& + \frac{m_b g_{LL}}{6M_{\tilde{t}_1}^2} f_{13}(R_{t_1}, R_b) + \frac{M_{\tilde{g}} g_{LL}}{6M_{\tilde{t}_1}^4} m_b X_b f_6(R_{t_1}, R_b) \\
& - \frac{m_t m_b X_b g_{RL}}{24M_{\tilde{t}_2}^4} (3f_{12}(R_{t_2}, R_b) - 2f_{15}(R_{t_2}, R_b)) \\
& - \frac{m_t m_b X_t g_{RL}}{M_{\tilde{t}_1}^2 - M_{\tilde{t}_2}^2} \left(\frac{f_{13}(R_{t_2}, R_b)}{6M_{\tilde{t}_2}^2} - \frac{f_{13}(R_{t_1}, R_b)}{6M_{\tilde{t}_1}^2} \right) \\
& + \frac{M_{\tilde{g}} m_t m_b X_t X_b g_{RL}}{(M_{\tilde{t}_1}^2 - M_{\tilde{t}_2}^2)} \left(\frac{f_6(R_{t_1}, R_b)}{6M_{\tilde{t}_1}^4} - \frac{f_6(R_{t_2}, R_b)}{6M_{\tilde{t}_2}^4} \right) \\
& - \frac{m_t^2 X_t g_{LR}}{M_{\tilde{t}_1}^2 - M_{\tilde{t}_2}^2} \left(\frac{f_{13}(R_{t_1}, R_b)}{6M_{\tilde{t}_1}^2} - \frac{f_{10}(R_{t_1}, R_b)}{3M_{\tilde{t}_1}^2} - \frac{f_{13}(R_{t_2}, R_b)}{6M_{\tilde{t}_2}^2} + \frac{f_{10}(R_{t_2}, R_b)}{3M_{\tilde{t}_2}^2} \right) \\
& - \frac{m_b^2 X_b g_{LR}}{12M_{\tilde{t}_1}^4} f_{15}(R_{t_1}, R_b) - \frac{M_{\tilde{g}} g_{LR}}{24M_{\tilde{t}_1}^4} (m_t^2 f_2 + M_{H^+}^2 f_3 + m_b^2 f_4)(R_{t_1}, R_b) \\
& - \frac{M_{\tilde{g}} m_b^2 X_b^2 g_{LR}}{12M_{\tilde{t}_1}^6} f_8(R_{t_1}, R_b) - \frac{M_{\tilde{g}} (M_L'^2 - M_R'^2) g_{LR}}{12M_{\tilde{t}_1}^4} f_6(R_{t_1}, R_b) \Bigg] , \tag{C.17}
\end{aligned}$$

C.4 Near-zero sbottom mixing and maximal stop mixing

The results for K_t , H_t , K_b and H_b up to order M_{EW}^2/M_{SUSY}^2 are:

$$\begin{aligned}
K_t &= \frac{\alpha_s}{3\pi} \left[\frac{M_{\tilde{g}} X_t}{M_S^2} f_1(R_t) + \frac{1}{2} \ln \frac{M_{b_1}^2}{M_S^2} - g_1(R_{b_1}) + g_1(R_t) - g_2(R_{b_1}) + g_2(R_t) \right. \\
&\quad - \frac{m_b^2 X_b^2}{(M_{\tilde{b}_1}^2 - M_{\tilde{b}_2}^2)^2} \left(-\frac{1}{2} \ln \frac{M_{\tilde{b}_2}^2}{M_{\tilde{b}_1}^2} + g_1(R_{b_2}) - g_1(R_{b_1}) + g_2(R_{b_2}) - g_2(R_{b_1}) \right) \\
&\quad - \frac{m_t^2}{12M_S^2} (2f_2 - f_3)(R_t) + \frac{m_t^2 X_t^2}{24M_S^4} (4f_2 - 2f_3 + f_4)(R_t) - \frac{M_L^2 - M_R^2}{12M_S^2} (3f_1 - f_2)(R_t) \\
&\quad \left. + \frac{M_{\tilde{g}} m_b^2 X_b}{M_{\tilde{b}_1}^2 - M_{\tilde{b}_2}^2} \left(\frac{f_2(R_{b_1})}{3M_{\tilde{b}_1}^2} - \frac{f_2(R_{b_2})}{3M_{\tilde{b}_2}^2} \right) - \frac{m_b^2}{6M_{\tilde{b}_1}^2} (2f_2 - f_3)(R_{b_1}) - \frac{m_b^2}{12M_{\tilde{b}_2}^2} (2f_2 - f_3)(R_{b_2}) \right] , \\
H_t &= -\frac{2\alpha_s}{3\pi} \frac{1}{m_t \cot \beta} \left[-\frac{M_{\tilde{g}} g_{RL}}{2M_S^2} f_1(R_t, R_{b_1}) + \frac{m_t g_{LL}}{6M_S^2} (2f_{10} - f_{13})(R_t, R_{b_1}) \right. \\
&\quad + \frac{M_{\tilde{g}} g_{LL}}{6M_S^4} m_t X_t f_5(R_t, R_{b_1}) + \frac{m_b g_{RR}}{6M_S^2} f_{13}(R_t, R_{b_2}) \\
&\quad + \frac{M_{\tilde{g}} m_b X_b}{M_{\tilde{b}_1}^2 - M_{\tilde{b}_2}^2} \left(g_{RR} - \frac{m_b X_b}{M_{\tilde{b}_1}^2 - M_{\tilde{b}_2}^2} g_{RL} \right) \left(\frac{f_1(R_t, R_{b_2})}{2M_S^2} - \frac{f_1(R_t, R_{b_1})}{2M_S^2} \right) \\
&\quad \left. - \frac{m_t m_b X_b g_{LR}}{6M_S^2 (M_{\tilde{b}_1}^2 - M_{\tilde{b}_2}^2)} (f_{13}(R_t, R_{b_1}) - 2f_{10}(R_t, R_{b_1}) - f_{13}(R_t, R_{b_2}) + 2f_{10}(R_t, R_{b_2})) \right]
\end{aligned}$$

$$\begin{aligned}
& - \frac{m_t m_b X_t g_{LR}}{24 M_S^4} f_{14}(R_t, R_{b_2}) + \frac{M_{\tilde{g}} m_t m_b X_t X_b g_{LR}}{6 M_S^4 (M_{\tilde{b}_1}^2 - M_{\tilde{b}_2}^2)} (f_5(R_t, R_{b_1}) - f_5(R_t, R_{b_2})) \\
& - \frac{m_t^2 X_t g_{RL}}{24 M_S^4} (3 f_{11}(R_t, R_{b_1}) - f_{14}(R_t, R_{b_1})) \\
& - \frac{m_b^2 X_b g_{RL}}{6 M_S^2 (M_{\tilde{b}_1}^2 - M_{\tilde{b}_2}^2)} (f_{13}(R_t, R_{b_2}) - f_{13}(R_t, R_{b_1})) \\
& - \frac{M_{\tilde{g}} g_{RL}}{24 M_S^4} (m_t^2 f_2 + M_{H^+}^2 f_3 + m_b^2 f_4)(R_t, R_{b_1}) - \frac{M_{\tilde{g}} m_t^2 X_t^2 g_{RL}}{12 M_S^6} f_7(R_t, R_{b_1}) \\
& - \frac{M_{\tilde{g}} (M_L^2 - M_R^2) g_{RL}}{12 M_S^4} f_5(R_t, R_{b_1}) \Big] \\
K_b = & \frac{\alpha_s}{3\pi} \left[- \frac{2 M_{\tilde{g}} X_b}{M_{\tilde{b}_1}^2 - M_{\tilde{b}_2}^2} \left(\ln \frac{M_{\tilde{b}_2}^2}{M_{\tilde{b}_1}^2} + g_1(R_{b_1}) - g_1(R_{b_2}) \right) - \frac{1}{2} \ln \frac{M_{\tilde{b}_1}^2}{M_S^2} + g_1(R_{b_1}) \right. \\
& - g_1(R_t) + g_2(R_{b_1}) - g_2(R_t) + \frac{m_b^2 X_b^2}{(M_{\tilde{b}_1}^2 - M_{\tilde{b}_2}^2)^2} \left(-\frac{1}{2} \ln \frac{M_{\tilde{b}_2}^2}{M_{\tilde{b}_1}^2} + g_1(R_{b_2}) - g_1(R_{b_1}) \right. \\
& \left. \left. + g_2(R_{b_2}) - g_2(R_{b_1}) \right) - \frac{m_b^2}{12 M_{\tilde{b}_2}^2} (2 f_2 - f_3)(R_{b_2}) \right. \\
& \left. - \frac{m_t^2}{4 M_S^2} (2 f_2 - f_3)(R_t) - \frac{m_t^2 X_t^2}{24 M_S^4} (4 f_2 - 2 f_3 + f_4)(R_t) + \frac{M_L^2 - M_R^2}{12 M_S^2} (3 f_1 - f_2)(R_t) \right. \\
& \left. - \frac{M_{\tilde{g}} m_t^2 X_t}{6 M_S^4} (2 f_3 - f_4)(R_t) \right], \\
H_b = & - \frac{2\alpha_s}{3\pi} \frac{1}{m_b \tan \beta} \left[- \frac{M_{\tilde{g}} g_{LR}}{2 M_S^2} f_1(R_t, R_{b_2}) + \frac{m_t g_{RR}}{6 M_S^2} (2 f_{10} - f_{13})(R_t, R_{b_2}) \right. \\
& + \frac{M_{\tilde{g}} g_{RR}}{6 M_S^4} m_t X_t f_5(R_t, R_{b_2}) + \frac{m_b g_{LL}}{6 M_S^2} f_{13}(R_t, R_{b_1}) \\
& + \frac{M_{\tilde{g}} m_b X_b}{M_{\tilde{b}_1}^2 - M_{\tilde{b}_2}^2} \left(g_{LL} + \frac{m_b X_b}{M_{\tilde{b}_1}^2 - M_{\tilde{b}_2}^2} g_{LR} \right) \left(\frac{f_1(R_t, R_{b_2})}{2 M_S^2} - \frac{f_1(R_t, R_{b_1})}{2 M_S^2} \right) \\
& - \frac{m_t m_b X_b g_{RL}}{6 M_S^2 (M_{\tilde{b}_1}^2 - M_{\tilde{b}_2}^2)} (f_{13}(R_t, R_{b_1}) - 2 f_{10}(R_t, R_{b_1}) - f_{13}(R_t, R_{b_2}) + 2 f_{10}(R_t, R_{b_2})) \\
& - \frac{m_t m_b X_t g_{RL}}{24 M_S^4} f_{14}(R_t, R_{b_1}) + \frac{M_{\tilde{g}} m_t m_b X_t X_b g_{RL}}{6 M_S^4 (M_{\tilde{b}_1}^2 - M_{\tilde{b}_2}^2)} (f_5(R_t, R_{b_1}) - f_5(R_t, R_{b_2})) \\
& - \frac{m_t^2 X_t g_{LR}}{24 M_S^4} (3 f_{11}(R_t, R_{b_2}) - f_{14}(R_t, R_{b_2})) \\
& - \frac{m_b^2 X_b g_{LR}}{6 M_S^2 (M_{\tilde{b}_1}^2 - M_{\tilde{b}_2}^2)} (f_{13}(R_t, R_{b_2}) - f_{13}(R_t, R_{b_1})) \\
& - \frac{M_{\tilde{g}} g_{LR}}{24 M_S^4} (m_t^2 f_2 + M_{H^+}^2 f_3 + m_b^2 f_4)(R_t, R_{b_2}) - \frac{M_{\tilde{g}} m_t^2 X_t^2 g_{LR}}{12 M_S^6} f_7(R_t, R_{b_2}) \\
& \left. + \frac{M_{\tilde{g}} (M_L^2 - M_R^2) g_{LR}}{12 M_S^4} f_5(R_t, R_{b_2}) \right]. \tag{C.18}
\end{aligned}$$

References

- [1] J. F. Gunion, H. E. Haber, Nucl. Phys. **B272**, 1 (1986); **B278**, 449 (1986) [E: **B402**, 567 (1993)]; J. F. Gunion, H. E. Haber, G. Kane, S. Dawson, *The Higgs Hunter's Guide* (Addison-Wesley, Reading, MA, 1990) [E: hep-ph/9302272].
- [2] H. E. Haber, G. L. Kane, Phys. Rept. **117**, 75 (1985).
- [3] S. Andriga *et al.* [ALEPH, DELPHI, L3 and OPAL Collaboration and the LEP working group for Higgs boson searches] (July, 2000), <http://lephiggs.web.cern.ch/LEPHIGGS/papers/>; P. Bock *et al.* [ALEPH, DELPHI, L3 and OPAL Collaborations and the LEP working group for Higgs boson searches], CERN-EP-2000-055 (April, 2000).
- [4] F. Abe *et al.* [CDF Collaboration], Phys. Rev. Lett. **79**, 357 (1997) [hep-ex/9704003]; B. Abbott *et al.* [D0 Collaboration], Phys. Rev. Lett. **82**, 4975 (1999) [hep-ex/9902028].
- [5] J. Guasch and J. Solà, Phys. Lett. B **416**, 353 (1998) [hep-ph/9707535]; J. A. Coarasa, J. Guasch, J. Solà and W. Hollik, Phys. Lett. B **442**, 326 (1998) [hep-ph/9808278].
- [6] M. Spira, Fortsch.Phys. 46 (1998) 203-284 [hep-ph/9705337].
- [7] A. C. Bawa, C. S. Kim and A. D. Martin, Z. Phys. C **47**, 75 (1990); V. Barger, R. J. Phillips and D. P. Roy, Phys. Lett. B **324** (1994) 236 [hep-ph/9311372]; S. Moretti and K. Odagiri, Phys. Rev. D **55** (1997) 5627 [hep-ph/9611374].
- [8] J. F. Gunion, Phys. Lett. B **322** (1994) 125 [hep-ph/9312201]; F. Borzumati, J. Kneur and N. Polonsky, Phys. Rev. D **60** (1999) 115011 [hep-ph/9905443]; D. J. Miller, S. Moretti, D. P. Roy and W. J. Stirling, Phys. Rev. D **61** (2000) 055011 [hep-ph/9906230].
- [9] A. Dobado, M. J. Herrero and S. Peñaranda, Eur. Phys. J. C **7** (1999) 313 [hep-ph/9710313]; In Barcelona 1997, *Quantum effects in the minimal supersymmetric standard model* 266-286, World Scientific, ed. J. Solà [hep-ph/9711441]; Eur. Phys. J. C **12** (2000) 673 [hep-ph/9903211]; Eur. Phys. J. C **17** (2000) 487 [hep-ph/0002134].
- [10] H. E. Haber, M. J. Herrero, H. E. Logan, S. Peñaranda, S. Rigolin and D. Temes, Phys. Rev. D **63** (2001) 055004 [hep-ph/0007006].
- [11] H. E. Haber, M. J. Herrero, H. E. Logan, S. Peñaranda, S. Rigolin and D. Temes, hep-ph/0102169. “Decoupling properties of MSSM particles in Higgs and top decays”. Invited talk given by M. J. H. at the RADCOR-2000 symposium, Carmel CA, USA, 11-15 September, 2000.

- [12] R. A. Jiménez and J. Solà, Phys. Lett. B **389**, 53-61 (1996) [hep-ph/9511292].
- [13] A. Bartl, H. Eberl, K. Hidaka, T. Kon, W. Majerotto and Y. Yamada, Phys. Lett. B **378**, 167 (1996) [hep-ph/9511385].
- [14] A. Méndez and A. Pomarol, Phys. Lett. B **252** (1990) 461; C. Li and R. J. Oakes, Phys. Rev. D **43** (1991) 855; A. Djouadi and P. Gambino, Phys. Rev. D **51** (1995) 218 [hep-ph/9406431].
- [15] T. Affolder *et al.* [CDF Collaboration], Phys. Rev. Lett. **84** (2000) 5704 [hep-ex/9910049].
- [16] R. Barate *et al.* [ALEPH Collaboration], Phys. Lett. B **499** (2001) 67 [hep-ex/0011047].
- [17] S. Abachi *et al.* [D0 Collaboration], Phys. Rev. Lett. **75**, 618 (1995); F. Abe *et al.* [CDF Collaboration], Phys. Rev. D **56**, R1357 (1997).
- [18] J.F. Gunion, H.E. Haber, G.L. Kane and S. Dawson, *SCIPIP-89-13* (1989)
- [19] A. Dabelstein, Z. Phys. C **67** (1995) 495 [hep-ph/9409375].
- [20] M. Carena, D. Garcia, U. Nierste and C. E. Wagner, Nucl. Phys. B **577** (2000) 88 [hep-ph/9912516]; H. Eberl, K. Hidaka, S. Kraml, W. Majerotto and Y. Yamada, Phys. Rev. D **62** (2000) 055006 [hep-ph/9912463].
- [21] W. Hollik, in *Precision Tests of the Standard Electroweak Model*, edited by P. Langacker (World Scientific, Singapore, 1995), p. 37–116.
- [22] A. Dobado, M. J. Herrero and D. Temes, in progress.
- [23] A. M. Curiel, M. J. Herrero, D. Temes and J. F. de Troconiz, in progress.